The United Nations University

GEOTHERMAL TRAINING PROGRAMME
Orkustofnun, Grensásvegur 9,
IS-108 Reykjavík, Iceland

Reports 1997
Number 6

THE USE OF SCHLUMBERGER SOUNDING IN GEOTHERMAL EXPLORATION WITH AN EXAMPLE FROM KRÍSUVÍK AREA, SW-ICELAND

Ha Ngoc Hung
Geological and Mineral Survey,
Hydrogeological Division No.2,
Nghiatan-Tuliem District, Hanoi,
VIETNAM

ABSTRACT

Resistivity methods have proved to be the most successful geophysical methods for geothermal exploration. The report briefly summarizes the use of resistivity methods for geothermal exploration. It then focuses on the widely used Schlumberger method and its comparison to the TEM method.

The usefulness of the Schlumberger method is demonstrated through interpretation of survey data from the Krísuvík geothermal area on the Reykjanes Peninsula, SW-Iceland. One-dimensional interpretation of 43 Schlumberger soundings reveals a resistivity structure reflecting the geothermal activity in the area.

1. INTRODUCTION

This report is a result of the six months course, at the UNU, Geothermal Training Programme, Orkustofnun in Iceland, 1997. The author attended an introductory lecture course covering geology, geophysics, borehole logging, reservoir engineering and utilization of geothermal resources and two geological excursions around Iceland. During the specialized geophysical course, the author was introduced to various kinds of geophysical methods applied in geothermal exploration such as resistivity, gravity, magnetic and seismic methods. The author has chosen to present the Schlumberger sounding method in his report with an example from the Krísuvík area in Southwest Iceland.

The Krísuvík (also written Krýsuvík) area is one of several high-temperature areas located on the Reykjanes Peninsula within the volcanic zone which crosses Iceland from southwest to northeast (Figure 1). Some reports have already been published about this area by Orkustofnun (e.g. Arnórsson et al., 1975; Orkustofnun and Vatnaskil Consulting Engineers, 1986) and UNU Fellows (e.g. Vargas, 1992). The purpose of the Schlumberger soundings discussed in this report is to locate and delineate the geothermal system in the area. Forty-three Schlumberger soundings and two TEM soundings are interpreted by the one-dimensional inversion programs SLINV and TINV. The results are presented in two resistivity cross-sections and five iso-resistivity maps in order to reveal the resistivity structure.

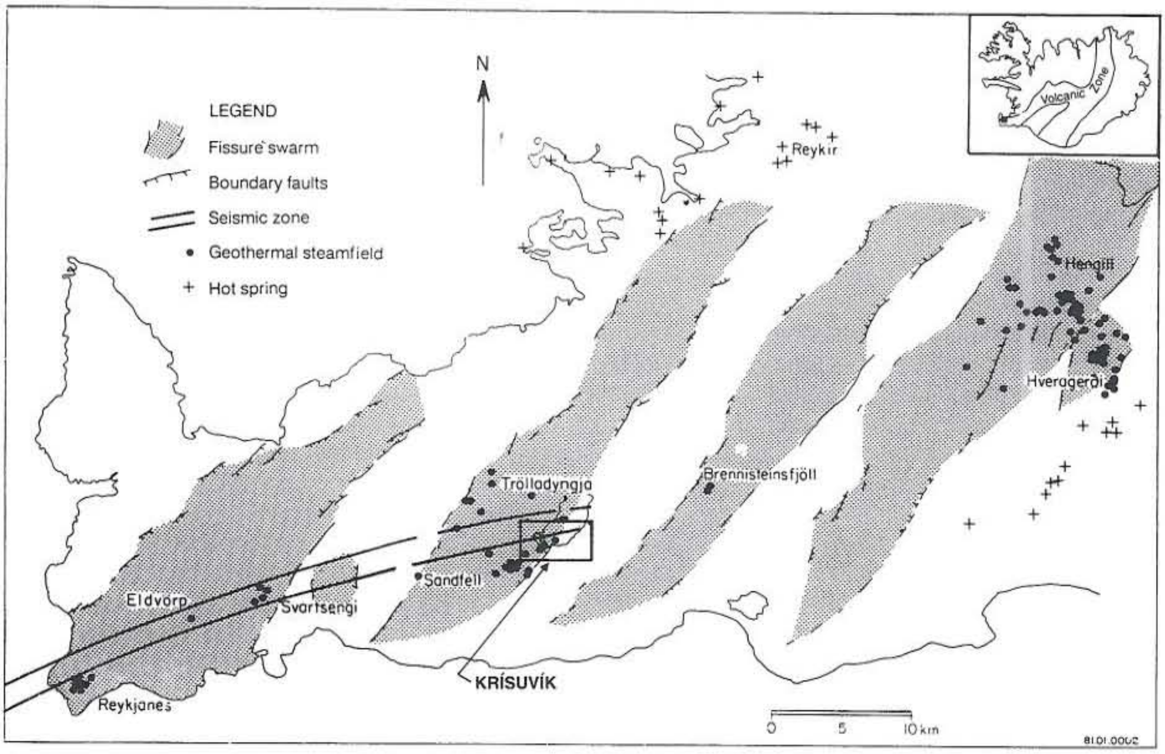

FIGURE 1: Volcanic systems and high-temperature areas of the Reykjanes Peninsula (modified from Saemundsson and Fridleifsson, 1980)

2. RESISTIVITY METHODS IN GEOTHERMAL EXPLORATION

2.1 General

Various resistivity methods have been used for exploring different types of geothermal systems. The effectiveness of these geophysical methods was greatly increased when emphasis was shifted from prospecting the geology and the structures that contain the geothermal fluids to prospecting the fluids themselves and concentrating on determining those parameters which are most sensitive to changes in temperature. Resistivity surveys are of particular importance in mapping temperature anomalies, faults, fractures, lithological contacts, thermal brine and zones of hydrothermal alteration. The importance of resistivity methods in geothermal exploration relies on the facts that the resistivity is the physical parameter which is most affected by thermal anomalies at depth and the resistivity of the subsurface rocks can be measured from the surface.

The aim of resistivity methods in geothermal exploration is to locate and delineate resistivity structures and relate them to hydrogeological and thermal structures associated with geothermal reservoirs. According to Hochstein and Soengkono (1995), resistivity surveys used for geothermal exploration can be broadly grouped into:

- Reconnaissance mapping. This is usually the first type of survey made to determine the gross resistivity features of geothermal prospects.
- Vertical electrical sounding (VES), involving a survey to determine the vertical resistivity structure.
- Location of steep boundaries, involving a follow-up to define the boundaries and internal structure of geothermal reservoirs.

In Iceland, direct current resistivity methods have been applied in geothermal exploration since 1949. Schlumberger soundings and head-on-resistivity profiling have been used extensively both in exploration for low-temperature geothermal resources outside the volcanic rift zone and for high-temperature resources inside the volcanic rift zone (Flóvenz, 1984). In recent years transient electromagnetic (TEM) soundings have been more favoured in exploration for high-temperature resources.

2.2 Overview of resistivity methods used in geothermal exploration

The various electrical methods used presently in geothermal exploration can be divided into DC-methods and EM-methods. In DC-methods, an artificial current source is used and the galvanic electrical field E is measured by a receiver circuit at a field station on the surface. To overcome the problem of steady natural potentials at the receiver side, a square wave (quasi DC) current of frequency lower than 1 Hz is usually injected into the ground through a pair of electrodes at the surface of the earth.

EM - methods are commonly divided into controlled source methods and natural source methods. In controlled source methods, an artificial electromagnetic field is induced in the ground and secondary fields are measured at the surface. If transient waveforms are used, the technique is referred to as time-domain or transient electromagnetic (TEM) technique. If a continuous sinusoidal waveform is used, the term frequency-domain technique is used. For each technique either a horizontal loop (magnetic dipole) or a grounded wire (electric dipole) can be used as a controlled source, and secondary E or B fields (or both) are measured by receiver circuits. For adequate depth penetration, energizing fields with frequency typically between 10 and 0.01 Hz are commonly employed in frequency domain techniques, which at present are used more often in geothermal exploration than time domain techniques. EM-methods using fields with frequencies greater than 200 Hz are rarely used because of their limited depth penetration (skin effect) in a low resistivity environment.

Natural source EM-methods use natural current fields induced in the earth by time variations in the earth's magnetic field. For frequencies <10 Hz the technique is known as magnetotelluric (MT) method; for higher frequencies the term audiomagnetolluric (AMT) method has been used. There is an overlap in the frequency range since modern MT equipment often allows recording of signals up to 1000 Hz.

2.3 Resistivity of rocks

2.3.1 Introduction

Electrical conductivity of a matter, σ, describes the ability of that matter to conduct electrical current. The reciprocal of conductivity is resistivity, ρ. It describes the ability to resist an electrical current. The unit of resistivity is Ωm. Resistivity of a matter is defined as the ratio of potential difference, ΔV, to current, I, across material which has a cross-sectional area A of 1 m^2 and a length L, 1 m.

$$\rho = \frac{\Delta V}{I}\frac{A}{L} \tag{1}$$

The resistivity of a body of fresh rock containing an electrolyte depends on the resistivity of the electrolyte and the temperature and to a lesser extent on the resistivity of the rock itself. The measured resistivity also depends on the porosity and the extent to which the voids are filled with electrolyte. In a geothermal field the electrolyte involved is the geothermal fluid and its resistivity is inversely related to the concentration of ions that it carries. The resistivity decreases with increasing temperature.

The electrical resistivity of rock depends on:

- Porosity and pore structure of the rock;
- Amount of water (saturation);
- Salinity of the water;
- Temperature and pressure;
- Alteration of the rock;
- Steam content in water.

The most important factors are the porosity, temperature, salinity of pore fluid and alteration minerals. In geothermal areas, the rocks are water-saturated. Ionic conduction in the saturating fluid depends on the number and mobility of ions and the connectivity of flow paths through the rock matrix. Usually, the saturating fluid is among the dominant conductors in the rock, and degree of saturation is of great importance to the bulk resistivity. The pressure dependence is negligible compared to the temperature dependence, provided it is sufficiently high so that there is no change in phase (Hersir and Björnsson, 1991). In the case of low-salinity fluids, the alteration minerals play a major role in the electrical conduction.

2.3.2 Porosity

Porosity is defined as the ratio between the pore volume and the total volume of a material. Pore spaces must be interconnected and filled with water in order that a rock may conduct electricity and most of the conduction takes place in the connecting pores. The resistivity of water-saturated rocks often varies approximately as the inverse square of the porosity. There are mainly three types of porosity:

- **Intergranular:** Porosity in sedimentary rocks is mainly intergranular;
- **Joints:** A net of fine fractures caused by tension and cooling of the rock, common in lava.;
- **Vugular porosity:** Big and irregular pores, formed as materials are dissolved and washed away or pores formed by gas.

An empirical relation, called Archie´s law, can be used to describe how resistivity depends on porosity if ionic conduction in the pore fluid dominates other conduction mechanisms in the rock (Archie, 1942). In normal rocks, Archie's law is valid if the resistivity of the pore fluid is of the order of 1 Ωm or less, but doubts are raised if the resistivity is much higher. Archie´s law can be stated as

$$\rho = \rho_w a \phi_t^{-n} \tag{2}$$

where

ρ = Bulk (measured) resistivity (Ωm);
ρ_w = Resistivity of the pore fluid (Ωm);
a = An empirical parameter; varies from less than 1 for intergranular porosity to over 1 for joint porosity, usually around 1;
n = Cementing factor, an empirical parameter, which varies from 1.2 for unconsolidated sediments to 3.5 for crystalline rocks, usually around 2;
ϕ_t = Porosity in proportions of total volume.

According to this law, the ratio ρ/ρ_w is constant for a given porosity. This ratio is called formation factor or *F*:

$$F = a\,\phi_t^{-n} = \rho/\rho_W \tag{3}$$

Permeability increases strongly with porosity, especially in fractured crystalline rocks. Since formation factor is a measure of porosity, it is also an inclined measure of permeability.

Typical resistivity values of different rock types in Iceland are shown in Tables 1 and 2.

TABLE 1: Typical resistivity of rocks in Iceland (Hersir and Björnsson, 1991)

Formation	**Resistivity [Ωm]**
Recent lava flows, above groundwater table	5,000-50,000
Dense intrusives (gabbro, dolerite)	10,000-15,000
Recent lava flows, below groundwater table	100-3,000
Basalts, rather dense	100-300
Palagonite	20-100
Low-temperature areas in basalt formations	30-100
Low-temperature areas in hyaloclastite formations	10-50
Rock with brine	5-15
High-temperature areas, freshwater	1-5
High-temperature areas, brine area	1-4

TABLE 2: Typical resistivity of several rock types

Rock types	**Resistivity [Ωm]**
Granite, ultrabasic, peridotite	1,000-3,000
Marble	400-1,000
Limestone, karstified	15-400
Gneiss	30-150
Sediments (depends on sand content)	10-100
Flyss with clay	low
Flyss with sand	high
Surface material with clay	low
Surface material with sand	high

2.3.3 Water-rock interaction and alteration

Archie´s law is only valid for conductive solutions (ρ_w<2 Ωm). The bulk resistivity is decreased by surface conduction along the interface between rock and water. By taking the interface conductivity into account, the total conductivity can be expressed as:

$$\sigma = \frac{1}{F}\sigma_w + \sigma_s' \tag{4}$$

where

F = Formation factor;
σ_s = Interface conductivity (1/Ωm);
σ_w = Conductivity of pore fluid (1/Ω/m).

The interface conductivity σ_s, is caused by fluid-matrix interaction. The interface conductivity depends more on the magnitude of the internal surface and on its connectivity than on the porosity. The two main reasons for interface conductivity are the presence of clay minerals (alteration) and surface double layer conduction.

In high-temperature geothermal areas in Iceland large variations in interface conductivity are caused by alteration of the rock matrix. The type of alteration minerals formed depends upon the temperature and the chemical composition of the fresh rocks and saturating fluid. Comparison of resistivity, on one hand, and temperature and alteration, on the other, has shown a good correlation for all high-temperature systems in Iceland (Árnason and Flóvenz, 1992). Cold (<50°C) and unaltered near-surface rocks have high resistivity (≥50-150 Ωm) where pore fluid conduction is probably dominant. In the temperature range of 50-200°C low resistivity (1-10 Ωm) is observed. This conductive cap is probably caused by conductive clay minerals, such as smectite, which are abundant in this temperature range. Deeper in the reservoir, where temperature is higher than 240°C, the conductive clay minerals are replaced by more resistive minerals, such as chlorite and epidote. The resistivity increases by about an order of magnitude and the pore fluid is probably the dominant conductor.

3. SCHLUMBERGER SOUNDING METHOD

3.1 Introduction

The Schlumberger sounding method was first applied by Conrad Schlumberger in 1912. It has for decades been widely and successfully used for detection and delineation of geothermal systems, location of aquifers, etc. The basic principle of the Schlumberger sounding method is to inject a current into the ground through current electrodes at the surface. This current creates a potential field in the ground. The subsurface resistivity can be inferred by measuring the resulting potential difference.

3.2 Theoretical overview

In the Schlumberger array, two potential electrodes and two current electrodes are positioned symmetrically along a straight line (Figure 2). The potential electrodes are placed at *M* and *N*. The distance between the potential electrodes *MN*, 2*P*, is kept much smaller than the distance between the current electrodes *AB* or 2*S* (at least five times smaller).

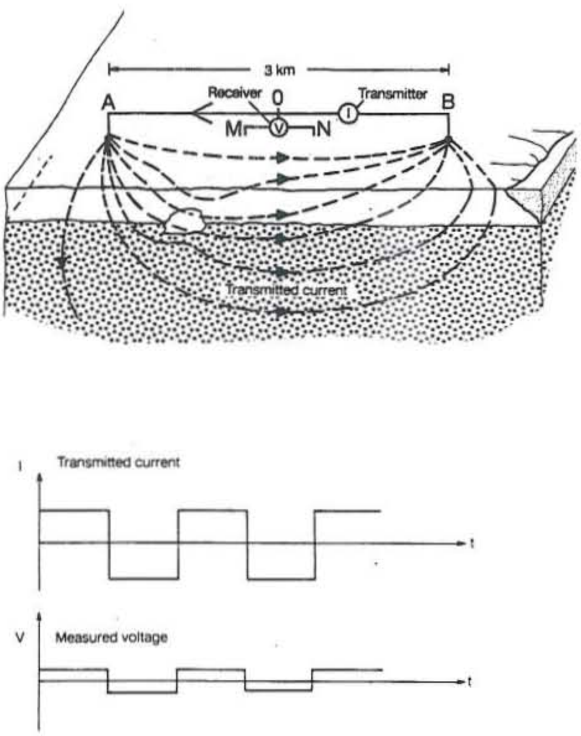

FIGURE 2: The Schlumberger sounding configuration (Hersir and Björnsson, 1991)

At the surface of a homogenenous and isotropic earth, the potential at a point at the distance r from a point of current injection is given as

$$V(r) = \frac{\rho I}{2\pi r} \tag{5}$$

where

V = Potential (V);
ρ = Resistivity (Ωm);
I = Current strength (A);
r = Distance from the current source to the measuring point (m).

For distances marked as in Figure 2 and the current I transmitted to the ground at A ($-I$ at B), the potential at N will be

$$V_N = V_N(A) + V_N(B) = \frac{\rho I}{2\pi(S+P)} + \frac{\rho(-I)}{2\pi(S-P)} = \frac{\rho I}{2\pi}\left(\frac{1}{S+P} - \frac{1}{S-P}\right) \tag{6}$$

The potential at M will be

$$V_M = V_M(A) + V_M(B) = \frac{\rho I}{2\pi(S-P)} + \frac{\rho(-I)}{2\pi(S+P)} \tag{7}$$

Hence, the potential difference becomes

$$\Delta V = V_M - V_N = 2\frac{\rho I}{2\pi}\left(\frac{1}{S-P} - \frac{1}{S+P}\right) = \frac{2\rho I P}{\pi(S^2 - P^2)} \tag{8}$$

This equation can be solved for ρ which can thus be calculated from the measured transmitted current and the corresponding measured potential difference. The resistivity for a homogeneous earth becomes:

$$\rho = \frac{\pi(S^2 - P^2)\Delta V}{2IP} \tag{9}$$

If the earth is not homogeneous the resistivity which is calculated from the measured values of the current and the potential is defined as the apparent resistivity, ρ_a, i.e. the resistivity a homogeneous earth would actually have to give those particular measured values for the current and the potential. Hence, the apparent resistivity is given by the following formula:

$$\rho_a = \frac{\Delta V}{I}\frac{\pi(S^2 - P^2)}{2P} \tag{10}$$

where

S = Half the current electrode spacing (AB/2);
P = Half the potential electrode spacing (MN/2).

To relate the measured apparent resistivity to the actual resistivity structure of a layered earth, it is necessary to express the voltage in terms of the relevant resistivity parameters. We consider the case of layered half space with N layers. Each layer is assumed homogeneous and isotropic with resistivity ρ_i and thickness d_i (the N^{th} layer is infinitely thick). The potential in the i^{th} layer, due to a current source at $r = 0$, $z = 0$ on the surface, is in cylindrical coordinates, given as

$$V_i(r,z) = \frac{\rho_i I}{2\pi} \int_0^\infty [C_i(\lambda) \cosh[\lambda(z-h_i)] + D_i(\lambda) \sinh[\lambda(z-h_i)]] \, J_o(\lambda r) \, d\lambda \tag{11}$$

where

r = Radial distance from the current source (m);
z = Depth below surface (m);
ρ_i = Resistivity of the layer (Ωm);
C_i *and* D_i = Functions of λ;
λ = Variable of integration;
h_i = Depth of the top of the i^{th} layer (m);
J_0 = Bessel function of order zero.

The C_i and D_i functions can be determined by imposing the following boundary conditions:

- The potential $V_i \to 0$ as $r \to 0$; for $i = 1, 2, 3 ...... N$;
- $V_N \to 0$ as $z \to \infty$;
- The potential V_i is continuous at each of the boundaries of the layers as: $V_i = V_{i+1}$ at $z = h_{i+1}$,
- The vertical current density is $J_z = 0$ at the surface layer, except at the current source,
- The vertical component of the current density is continuous at the boundary of the layers, i.e. at $z = h_{i+1}$,

$$\frac{1}{\rho_i} \frac{\partial V_i}{\partial z} = \frac{1}{\rho_{i+1}} \frac{\partial V_{i+1}}{\partial z} \tag{12}$$

These conditions imply that $D_N = -C_N$ at the N^{th} layer. Defining the kernel function $K_i = -C_i / D_i$, we have $K_N = 1$ and K_i is given by the recurrence relationship

$$K_i = \frac{K_{i+1} + \frac{\rho_i}{\rho_{i+1}} \tanh(\lambda d_i)}{\frac{\rho_i}{\rho_{i+1}} + K_{i+1} \tanh(\lambda d_i)} \tag{13}$$

where ρ_i and d_i are the resistivity and thickness of the i^{th} layer. For the uppermost layer, it can be shown that $D_1 = -1$ and therefore

$$V_1(r,z) = \frac{\rho_1 I}{2\pi} \int_0^\infty [K_1 \cosh(\lambda z) - \sinh(\lambda z)] \, J_0(\lambda r) \, d\lambda \tag{14}$$

At the surface, $z = 0$, this equation becomes

$$V_1(r) = \frac{\rho_1 I}{2\pi}\int_0^{\infty} K_1 J_0(\lambda r)\, d\lambda \tag{15}$$

Equation 15 along with the recurrence relationship as shown in Equation 13, give the potential at distance r from a point current source injecting the current I at the surface of a layered half space. Equation 15 can be used to calculate the potentials V_N and V_M in the Schlumberger array and therefore the apparent resistivity for a given layered earth.

3.3 Field procedure

In resistivity surveys the field procedure depends on the type of electrode configuration used. In the Schlumberger array, four electrodes are symmetrically positioned along a straight line. The distance between the current electrodes (*AB*) is considerably larger than that of the potential electrodes (*MN*). The distance between the current electrodes is increased in certain steps and measurements are made for each separation. The distance between the current electrodes is increased exponentially, usually with 10 steps per decade. In Iceland the starting length of half the current electrode spacing (*AB*/2) is usually 2.51 or 10 m, and the maximum spacing is usually 1780 m, but sometimes as high as 3000 m. As current electrode spacing increases the potential signal decreases. Therefore, half the potential electrode spacing (*MN*/2) is increased in steps, from 1 to 100 m.

By increasing the current electrode spacing, the current penetrates deeper into the earth and information is obtained on resistivity at greater depths. When the apparent resistivity has been calculated it is plotted as a function of half the current electrode spacing on a log-log paper and is ready for interpretation.

It takes 4 people to carry out a Schlumberger sounding. One controls the instruments, one writes down the results and plots the apparent resistivity curve. Two people move the current electrodes in each direction. At each point they push the electrodes into the ground and connect them to the transmitter cable, then the measurement at that point takes place. At the end of the sounding, a check for current leakage is made, one current electrode is disconnected, and high voltage is put on the transmitter cable and the potential between *M* and *N* measured as well as the transmitted current; this is made for both electrodes. If the measured potential sign is about 10% of the signal obtained when both current electrodes are connected or higher, something is wrong and has to be repaired.

3.4 Instrumentation

The equipment necessary for making Schlumberger soundings consists of a transmitter unit for introducing the current into ground and a receiver unit for measuring the corresponding potential difference. The instruments used in Iceland are designed and made by the electronic laboratory at Orkustofnun in cooperation with the company Örtölvutaekni.

The transmitter contains components like power supply, control module and 4 converters and measuring module as well as buttons, switches and metres on the front panel. The transmitter runs on 24 volts DC, and transmits a square wave of adjustable frequency. The output power is 500 W.

The receiver consists of a microprocessor module, handheld terminal and three differential input amplifiers. The advantage of having three independent amplifiers is higher efficiency in the measurements by simultaneously measuring the potential difference at the different potential electrode spacings. The microprocessor module is specially designed for this kind of resistivity measurements. The relevant values appear on the terminal as soon as they reach the module i.e. the transmitted current, the measured potential difference between the potential electrodes, the number of measurements made, their mean value and the standard deviation. Each value of the potential difference is, thus, a mean value of several measurements. In difficult conditions a few such mean values are collected for measuring one point. Finally, a weighted mean value is obtained from all the mean values where the weighing is determined by the standard deviation in each case. The microprocessor then uses the final potential value for determining the apparent resistivity at that point and the results appear on the terminal.

The wire used as a connector to the current and potential electrodes is a copper wire, 0,5 mm^2 in cross-section with a PVC-insolation. The first 120 m of the current transmitting wire are screened. This is done to reduce capacitive and inductive coupling where current wires and potential wire lie parallel. The screen of the current wire is connected to the frame of the transmitter. The unscreened part of the current wire is kept on reels, three 500 m reels for each half of the current dipole. To prevent leakage, the reels are put in solid plastic bags at the connection and the innermost reels are fastened to a stick so that they do not touch the ground.

The current electrodes are approximately 50 cm long aluminum poles. For AB/2 less than 600 m only one pole is used for each current electrode. With increasing dipole length or high contact resistance between the pole and the earth, the number of poles is increased.

The potential electrodes are 12 cm long copper sticks submerged in saturated copper-sulfate solution in a holder with a permeable ceramic tip. The contact between the electrode and the earth occurs as the solution seeps through the tip.

4. CENTRAL-LOOP TRANSIENT ELECTROMAGNETIC (TEM) METHOD

4.1 Introduction

As previously mentioned, the Schlumberger sounding method of electrical surveying has been the most common method used in geothermal exploration. However, many high-temperature geothermal areas are located in volcanic zones where large parts of the surface can be covered with lava making current injection into the earth almost impossible, such that the use of Schlumberger sounding is very difficult and time consuming.

In Iceland, the use of the central-loop transient electromagnetic method (TEM) is replacing the conventional Schlumberger sounding in geothermal exploration of areas of resistive surface conditions. Although the inversion of the sounding results, in terms of subsurface resistivity structure, is more complicated for the TEM-soundings than for Schlumberger soundings, experience in Iceland has shown that the TEM method is, in many respects, superior to the conventional Schlumberger soundings (Árnason, 1990).

4.2 Theoretical overview

In the central-loop TEM sounding method, the current in the earth is generated by a time varying magnetic field (Figure 3). It is different from the magnetotelluric method (MT) in that the magnetic field is not randomly varying but a field of a controlled magnitude generated by a source loop. A loop of wire is placed on the ground and a constant magnetic field of known strength is built up by transmitting a constant current in the loop. The current is then abruptly turned off. The decaying magnetic field induces electric current in the ground. The current distribution in the ground induces a secondary magnetic field decaying with time. The decay rate of the secondary magnetic field is monitored by measuring the voltage induced in a receiver coil (or a small loop) at the centre of the transmitter loop. The current distribution and the decay rate of the secondary magnetic field depend on the resistivity structure of the earth. The decay rate, recorded as a function of time after the current in the transmitter loop is turned off, can be interpreted in terms of the subsurface resistivity distribution. The depth of penetration in the central-loop TEM soundings is dependent on the geoelectrical section and on how long the induction in the receiver can be traced in time before it is drowned in noise.

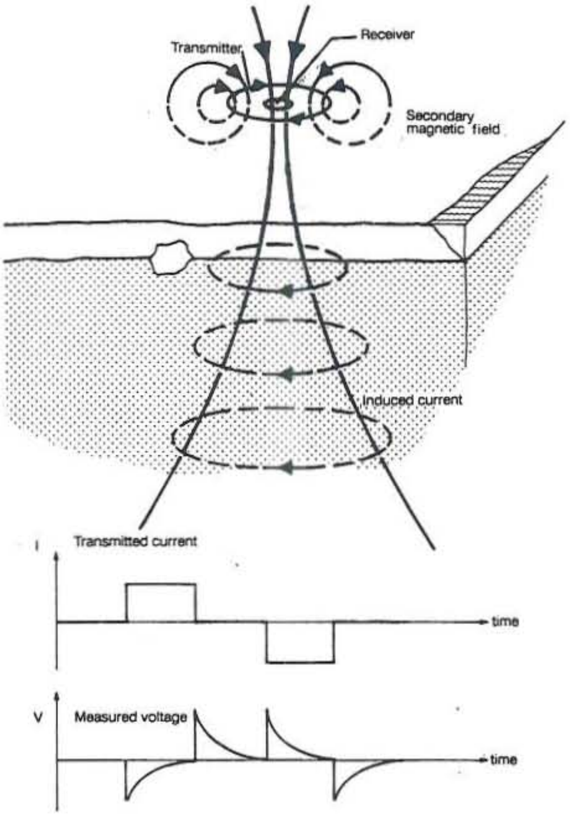

FIGURE 3: TEM sounding configuration (Hersir and Björnsson, 1991)

If a current I transmitted in a circular source-loop of radius r is abruptly turned off at $t = 0$, the induced voltage in a receiver coil at the centre of the loop is given, as a function of time, by

$$V(r,t) = A_r n_r A_s n_s \frac{I\mu_0}{\pi^2 r^3} \int_0^\infty Re[E^e(r,\omega)] \cos(\omega t)\, d\omega \tag{16}$$

where

t = Time passed since the current in the transmitter loop was turned off (s);
A_r = Area of the receiver coil (m^2);
n_r = Number of windings in the receiver coil;
μ_0 = Permeability of free space;
A_s = Area of the current loop (m^2);
n_s = Number of windings in the current loop;
$V(r,t)$ = Transient voltage (V);
$E^e(\omega,r)$ = Earth response factor.

The earth response factor $E^e(\omega,r)$ which is a function of angular frequency ω and the source loop radius r is given as

$$E^e(\omega,r) = 2r^2 \int_0^\infty \lambda \frac{S_0}{S_0 - T_0} J_1(\lambda r)\, dr \tag{17}$$

S_0, T_0 contain the parameters of the layered earth and are determined by recurrence relationships similar to Equation 13.

The so-called late time apparent resistivity is defined as

$$\rho_a(r,t) = \frac{\mu_0}{4\pi}\left[\frac{2\mu_0 A_r A_s n_s I}{5t^{5/2}V(r,t)}\right]^{5/2} \tag{18}$$

The sounding results are normally presented by late time apparent resistivity as a function of time according to Equation 18, where $V(r,t)$ is the measured induction in the receiver coil.

5. RESISTIVITY INTERPRETATION

5.1 Introduction

If the earth is divided into horizontal layers of infinite extent and the layers are electrically homogeneous and isotropic, the resistivity structure below a measuring site can be derived from the measured apparent resistivity. In this case, resistivity change is assured to occur only in one direction, i.e. with depth. One-dimensional interpretation of resistivity data is based on the assumption that the earth under the sounding site consists of horizontal resistivity layers.

Interpretation of measured resistivity data in terms of layered earth models can, in principle, be done by forward modelling. Forward modelling consists of guessing a layered structure and comparing the calculated response of the model to the measured resistivity data. By visual inspection of the difference between the measured and calculated response, a new model is guessed. This is continued until satisfactory agreement is obtained and the resulting model is taken as the interpretation of the measured curve.

One-dimensional interpretation is nowadays usually done by inversion programs. An inversion program contains a forward algorithm and an inversion algorithm (Árnason and Hersir, 1988). The inversion algorithm is a procedure that calculates, from the difference between calculated response of a given model and measured data, adjustment to the model parameters such that better agreement is obtained. This is normally done by calculating how a slight change in each of the model parameters effects the response. This can be used to determine changes in the parameters which results in better agreement with the measured response.

5.2 The inversion program SLINV

In the early days, one-dimensional interpretation of Schlumberger soundings was made with the help of apparent resistivity curves, but computer programs have long since replaced these. At the UNU Geothermal Training Programme in Iceland, a one-dimensional inversion program SLINV (Schlumberger Inversion) is used. This program was written and installed on PC computers by the Orkustofnun staff (Árnason and Hersir, 1988).

SLINV is a non-linear least-square program for inversion of Schlumberger soundings. The program uses an interactive Levenberg-Marquardt inversion algorithm described by Johansen (1977) together with a forward routine based on the linear filter method. The program consists of ten source files, the main program SLINV.FOR and nine subroutines.

The inversion program SLINV, like most inversion programs, works in such a way that it reads the measured data points (apparent resistivity curve) and prompts for a starting model. The interpreter guesses by visual inspection of the data curve, the number of layers and initial model parameters (resistivity values and thicknesses of the layers). The program then interactively adjusts the resistivity values and layer thicknesses to get the best fit between the measured curve and the curve calculated from the model. It is important to realize that the program does not change the number of layers during the interaction process.

It is therefore, in most cases, necessary to check models with different numbers of layers to find the model that best fits the data. It is advisable to keep the models simple and the number of layers as few as possible. It should also be kept in mind that the model resulting from inversion can depend on the initial guess and a bad initial guess can lead the inversion process astray. One feature of the program is that a layer parameter, i.e. resistivity or thickness of any layer in a model, can be fixed during the interaction process. The fixed parameter values determined manually may come from some geological concepts or the values may simply be known already from other studies.

The program calculates the apparent resistivity values from the given one-dimensional model using the gradient approximation. From Equations 10 and 15, it is seen that in the gradient approximation ($P<<S$), the apparent resistivity is given as a function of $r = AB/2$ by the following formula:

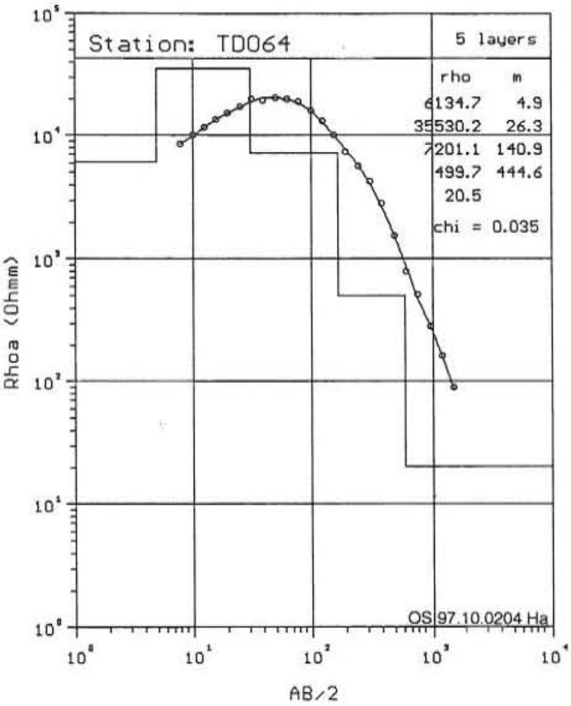

FIGURE 4: One-dimensional interpretation of Schlumberger sounding TD064 from Krísuvík area using the program SLINV

$$\rho_a(r) = \rho_1 r^2 \int_0^\infty K_1(\lambda) J_1(\lambda_r) \lambda \, \partial\lambda \tag{19}$$

The kernel function $K_1(\lambda)$ contains the model parameters and is given by the recurrence relationship (Equation 13). An example of one-dimensional interpretation of a Schlumberger sounding using the SLINV program is shown in Figure 4.

5.3 The inversion program TINV

A non-linear least-square inversion program, TINV, has been used for one-dimensional inversion of TEM soundings (Árnason, 1989). The program TINV is very similar to the program SLINV described above except for the forward algorithm calculating the central-loop TEM response of a given layered model. The program assumes that the field data is collected with equipment where the transmitted current is turned off linearly from maximum to zero and that the time values, at which the apparent resistivity values are given, are equally spaced in logarithm of time after the current has become zero. This program assumes that data is collected with a circular loop. If this is not the case the actual transmitter loop is simulated by a circular loop having the same area. An example of one-dimensional inversions of a TEM sounding using the TINV program is shown in Figure 5.

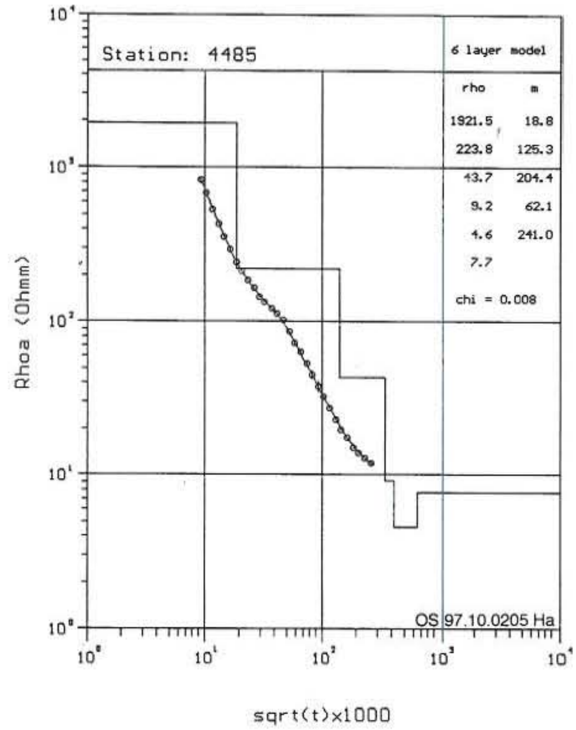

FIGURE 5: One-dimensional interpretation of TEM sounding T4485 from Krísuvík area using the TINV program

5.4 Factors affecting resistivity data

There are a number of systematic errors which can cause distortions of resistivity sounding curves and a scatter of the ρ_a data so that in the extreme case, no meaningful sounding curve can be constructed. Similar errors also occur during resistivity traverses which are often not noticed, whereas a single erroneous value of ρ_a can immediately be recognized in a sounding curve. Therefore, sounding data should always be plotted in the field, and suspect data should be rejected and repeated.

Errors can be caused by topographic effect, inhomogeneity and anisotropy and near-surface inhomogeneities, etc.

Topographic effects. Geothermal exploration is often carried out in mountainous terrain where topography can produce false resistivity anomalies. Knowledge of the nature of these effects and their inclusion in the interpretation models are important. Treatment of the raw resistivity data obtained from these rugged areas could produce topography- related anomalies that may lead to ambiguities in the interpreted models if one does not take into account the significance of topographic effects. Topographic effects are geometric effects which are inherent to the relative locations of the terrain itself where resistivity measurements are carried out. Because of these conditions; current flow lines are distorted with the corresponding effect on equi-potential lines. Thus the actual voltage readings get distorted which can be critical to field measurements and data interpretation. Higher ΔV values would be observed when the potential electrodes are placed perpendicular to the axis of a steep valley as compared to what would be observed over a horizontal free surface. This is caused by the "focussing" effect of the valley or the convergence of equi-potential lines. And the opposite effect is observed over high-angle ridges where divergence of equi-potential surfaces is normal to the current flow (Figure 6).

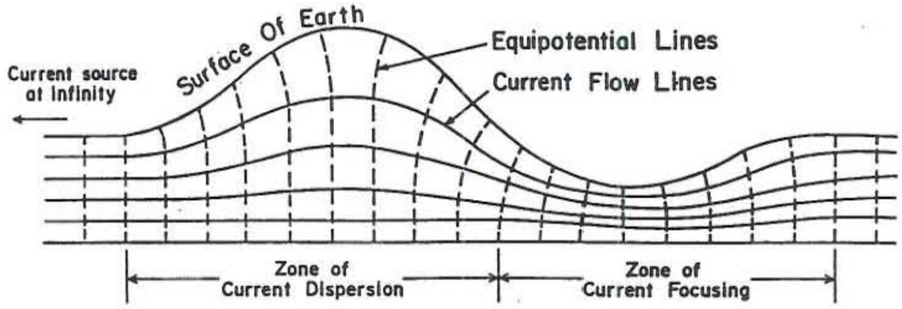

FIGURE 6: The effect of topography on current flow and equi-potential lines (Fox et al.,1978)

Near-surface inhomogeneities: When the depth of investigation is increased in Schlumberger soundings, the current electrodes *A* and *B* are moved symmetrically outwards from the centre, while keeping the distance between the potential electrodes *M* and *N* fixed. When the ratio of *AB/MN* becomes so large that the potential drop across *MN* becomes too small to be measured with reasonable accuracy, it becomes necessary to increase the distance between *M* and *N*. The apparent resistivity curve, therefore, contains overlapping segments for different *MN*. These segments often fail to tie in and are shifted (on log-scale) relative to each other.

"Shifts" in the apparent resistivity curves of Schlumberger soundings have been studied by Árnason (1984). These "shifts" are found to be of two categories: converging and constant (Figure 7) when the current electrode spacing is increased. Converging shifts are caused by large resistivity contrasts between layers in horizontally stratified earth. These shifts contain information about horizontally stratified resistivity structures. Non-converging shifts are caused by lateral resistivity variations at the centre of the Schlumberger sounding. The segments measured with shorter potential electrode spacings should be shifted so that they tie in with the segment measured with the largest potential electrode spacing.

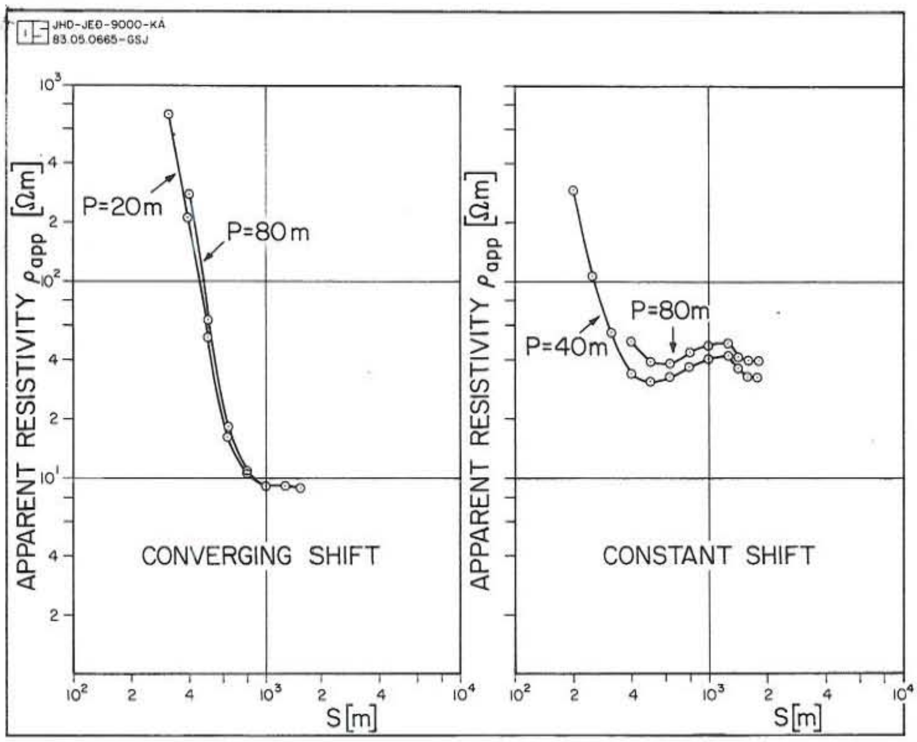

FIGURE 7: Shifts in apparent resistivity curves (Árnason 1984)

Inhomogeneity and anisotropy: One-dimensional interpretation is based on the assumption that the subsurface consists of a sequence of distinct layers of finite thickness separated by horizontal boundary planes, with the deepest layer extending to infinite depth. Each of these layers is assumed to be electrically homogeneous and isotropic. In practice, the assumption of homogeneity holds true if the contrast of resistivities of the geological structures within the layer is not too large. The magnitude of the electric anomalies of a non-homogeneous earth depends upon the resistivity differences between different rocks. In reality geological sequences may also be electrically anisotropic. For example, in formations made of many thin layers of different resistivity, the electrical resistivity is the same in all directions along a layer but different perpendicular to the stratification.

6. INTERPRETATION OF RESISTIVITY DATA FROM THE KRÍSUVÍK AREA

6.1 Introduction

The Krísuvík high-temperature field is one of several high-temperature areas on the Reykjanes Peninsula. The area is approximately 40 km^2 in the central part of the Reykjanes Peninsula, overlain by two ridges with a valley in between. Geothermal activity is manifested with steam vents, hot springs and highly altered rocks due to acid surface leaching. Some surveys have already been carried out such as geological, geophysical and geochemical surveys by Orkustofnun and UNU fellows.

A resistivity survey comprising 80 Schlumberger soundings and several resistivity profiles has been carried out in Krísuvík field (Orkustofnun and Vatnaskil Consulting Engineers, 1986; Georgsson, 1987) showing a rather complex structure with widespread low-resistivity layers ($<5\Omega$m) at 300 m below sea level and high-resistivity layers ($>10,000$ Ωm) at the surface. Borehole data show temperature with inverse gradient and with the highest temperature of 262°C. There is considerable discrepancy between measured temperatures and those from geochemical analysis of fumarolic gases. Various models have been proposed to try and explain the inverse temperature gradient. None of these, however, seems to be consistent with most of the observed characteristics of the geothermal field.

6.2 Geological information

The Reykjanes Peninsula belongs to the volcanic rift zone which crosses Iceland from southwest to northeast. There are Postglacial lava fields with steep-sided volcanic ridges which protrude through the lava fields. Rifting and transform fault characteristics can be seen. There have been many volcanic eruptions in the Krísuvík area giving rise to volcanic edifices on fissures. The Krísuvík high-temperature area is characterised by two major southwest-striking hyaloclastite ridges. The valley between the two ridges is covered with lava flows and most of the geothermal activity is found within the hyaloclastite ridges and on their outer sides but none in the lava covered valley between the two ridges. The fissure swarm that cuts the Krísuvík area is more intense at the ridges than in the valley; therefore, there has been more tectonic activity in zones occupied by the ridges than by the young lavas in the valley.

The thermal water in the Krísuvík area is highly saline, approaching 20,000 ppm Cl in the southern part, decreasing landwards as a result of the decreasing incursion of sea water into the geothermal system through the permeable volcanic strata. The seawater seems to percolate through the highly permeable bedrock and mix with the thermal waters of the geothermal system at Krísuvík area.

6.3 Location and interpretation of the resistivity soundings

The data presented here were collected by Orkustofnun in 1986. They comprise 43 Schlumberger soundings. The Schlumberger data are interpreted as an isolated data set since limited time did not allow comparison and inclusion of other resistivity data from the area, except that two recent TEM soundings (from 1997) are compared to nearby Schlumberger soundings. The location of the Schlumberger soundings (in UTM coordinates) and elevation is given in Table 3 and of the TEM soundings in Table 4. The station locations are also shown in Figure 8. TEM sounding T4687 is close to Schlumberger sounding TD084, and TEM sounding T4485 is close to TD080.

The Schlumberger data were interpreted by the one-dimensional inversion program SLINV. The final model is obtained when the average difference between measured and calculated values becomes of the order of a few percent. The sounding curves, the interpreted data curves and the resulting layered models, resistivity values and layer thicknesses are shown in Appendix I. The TEM soundings are in Appendix II. The results are also presented in two resistivity cross-sections and five iso-resistivity maps.

TABLE 3: Coordinates and elevation of Schlumberger soundings in Krísuvík

Sounding No.	UTM		Elevat. (m a.s.l.)	Sounding No.	UTM		Elevat. (m a.s.l.)
	X-coord.	Y-coord.			X-coord.	Y-coord.	
TD092	42350	89500	180	TD090	43500	88800	170
TD085	44300	88300	200	TD088	45250	47900	185
TD084	46100	87000	185	TD086	47400	86200	300
TD074	48150	85800	170	TD083	48450	85800	150
TD075	49250	85150	230	TD076	49700	84850	165
TD081	50300	84500	230	TD087	46850	86500	280
TD082	48800	85350	180	TD078	48150	85800	170
TD094	51200	90200	30	TD095	49900	88500	150
TD093	50650	89400	170	TD096	49350	88000	165
TD097	48800	86800	150	TD066	41100	87400	195
TD064	40110	90000	230	TD065	41200	91850	170
TD067	39050	91650	180	TD068	39750	85800	90
TD069	41100	85250	110	TD071	44100	88800	130
TD072	43300	86400	180	TD073	41100	83400	150
TD077	42100	84850	150	TD079	39500	84000	110
TD080	44400	85400	120	TD089	47400	88750	180
TD091	49850	87250	8	TD098	49400	86750	100
TD100	49000	86750	120	TD103	50650	86450	220
TD104	44650	81850	100	TD105	47300	82500	120
TD107	39250	80700	25	TD108	50500	81250	25
TD109	42800	79900	40	TD110	39100	81500	10
TD099	49850	86700	150				

TABLE 4: Coordinates and elevation of TEM soundings

Sounding No.	UTM		Elevat. (m a.s.l.)
	X-coord.	Y-coord.	
T4687	45900	87050	185
T4485	44300	85300	180

6.4 Results of one-dimensional interpretation

Resistivity cross-section I (Figure 9). The cross-section is 12 km long (see Figure 8) and runs NW-SE crossing the two main volcanic ridges. Thirteen soundings are projected into the profile, showing the following main features.

A clear resistivity anomaly, consisting of a low-resistivity cap and a more resistive inner core is observed and reflects geothermal activity. The anomaly has a very sharp boundary to the east, south of Lake Kleifarvatn, but no well defined western boundary is observed on the section. The resistivity anomaly

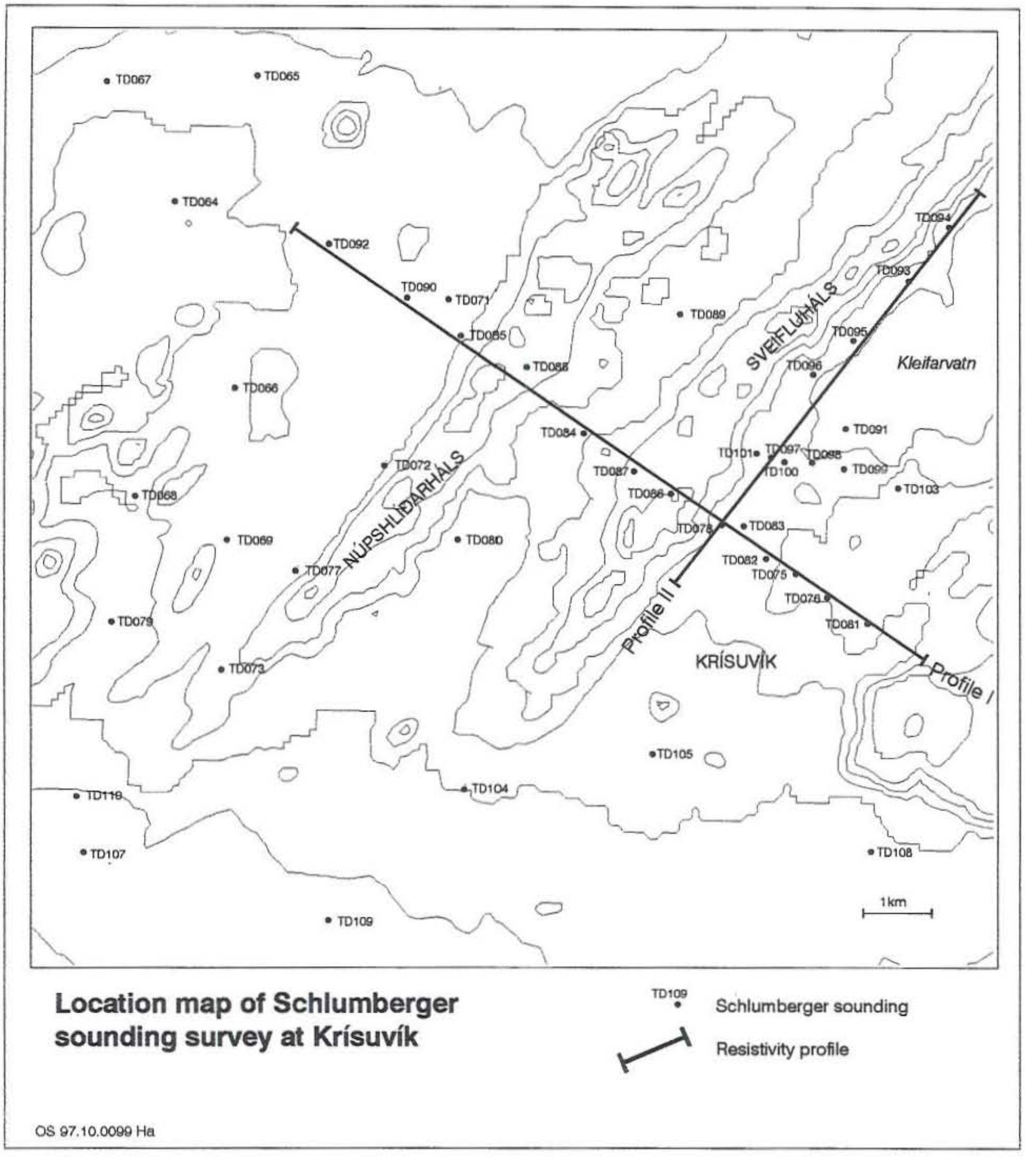

FIGURE 8: Location of Schlumberger soundings in the Krísuvík area

rises up under the two hyaloclastite ridges, Núpshlídarháls and Sveifluháls to the south of Kleifarvatn. This is probably an indication of upflow along tectonic fissures under the ridges. A second shallow low-resistivity layer is observed south of Kleifarvatn. This probably reflects lateral flow of hot water from northwest.

Resistivity cross-section II (Figure 10). This cross-section is 8 km long, trending from southwest to northeast, between Sveifluháls and Lake Kleifarvatn with 7 soundings placed on it. The following aspects are observed in this profile.

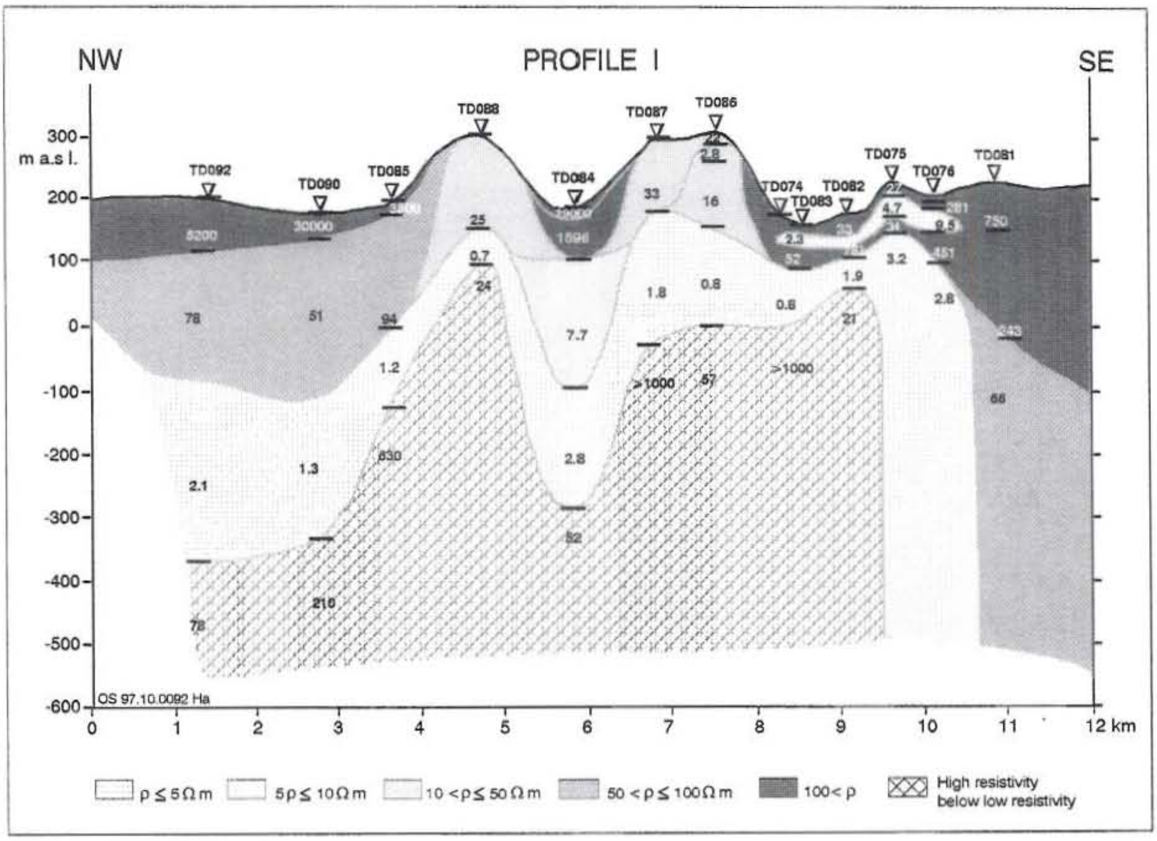

FIGURE 9: Resistivity cross-section I

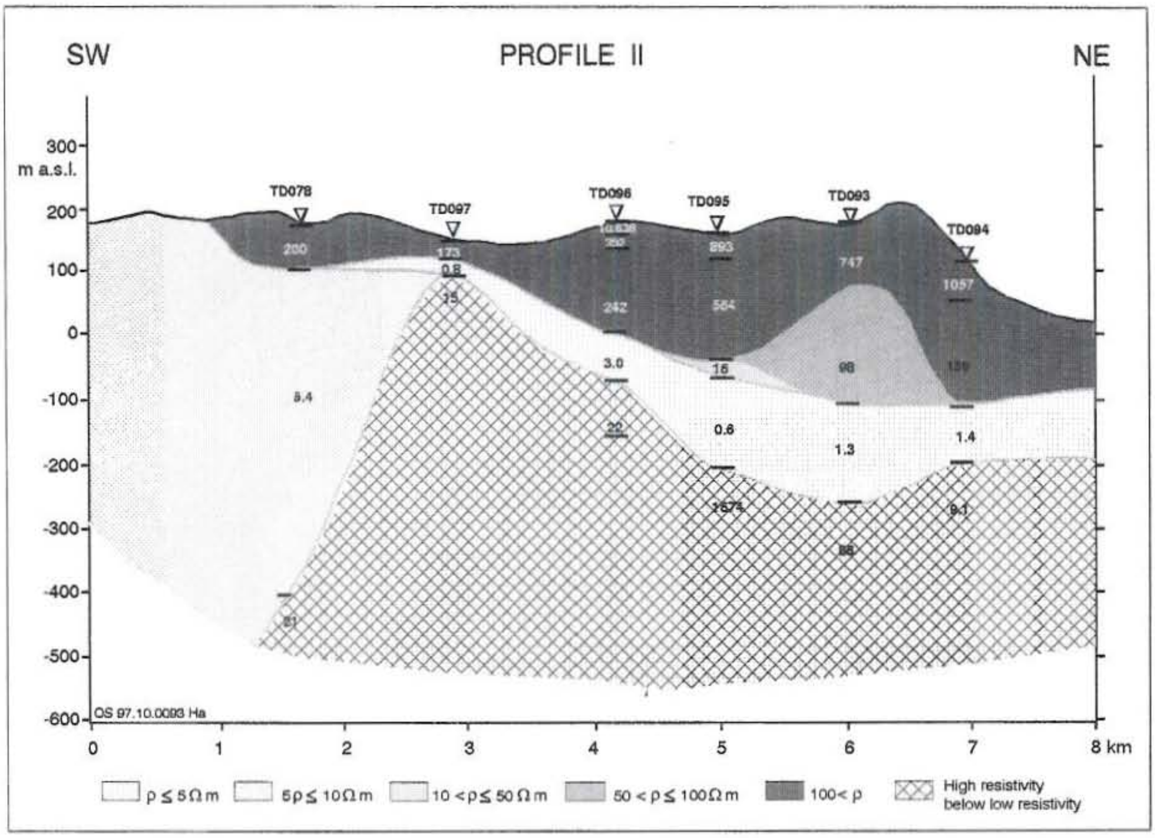

FIGURE 10: Resistivity cross-section II

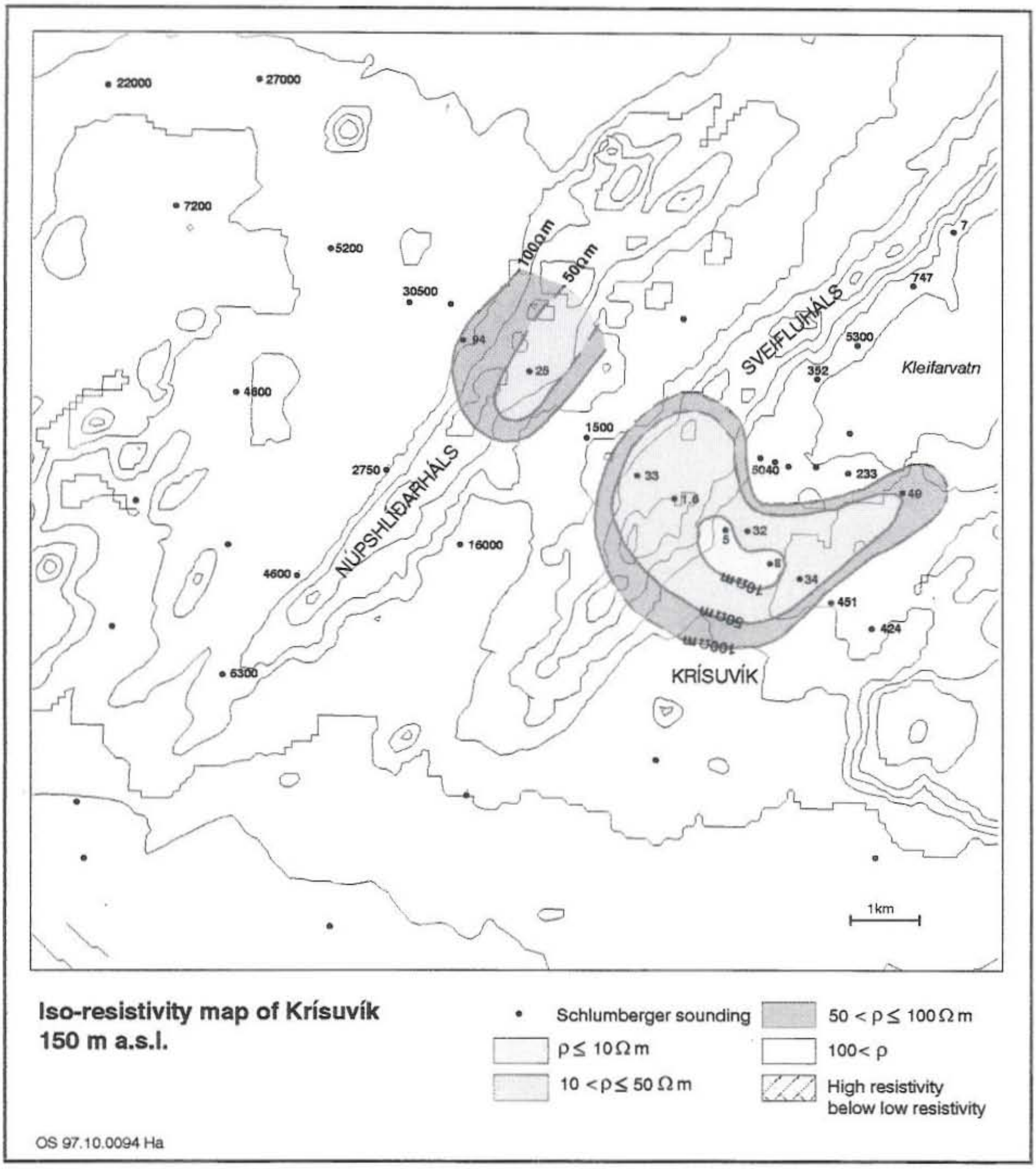

FIGURE 11: Iso-resistivity map of the Krísuvík area at 150 m above sea level

A clear low-resistivity cap and underlaying high-resistivity core dominate. Under the northern part of the section, low resistivity is found at about 100 m below sea level. It comes up towards the south and is close to the surface (100 m above sea level) under sounding TD097 just south of Kleifarvatn. Further south, the depth to the resistive core increases rather sharply and a thick low-resistivity layer is seen. This is probably because the southern part of the section is close to the eastern boundary of the geothermal system.

Iso-resistivity map at 150 m a.s.l. (Figure 11). This map shows two low-resistivity anomalies. One is under the northern part of Núpshlídarháls. The northern boundary of this anomaly is not defined because of lack of data. The other anomaly is under Sveifluháls, southwest of Lake Kleifarvatn and stretches to the east, south of the lake. These anomalies can be assumed to indicate the top of two separate upflow zones.

Iso-resistivity map at sea level (Figure 12). At this depth a continuous low-resistivity anomaly is seen between the two separate anomalies of the previous map which now are starting to appear as higher resistivity below low-resistivity. This might indicate a NW-SE trending structure at depth connecting the upflow areas. To the north of the low-resistivity anomaly, relatively low-resistivity is observed. The northern, as well as the southern, margins of the anomaly are not well defined because of limited data.

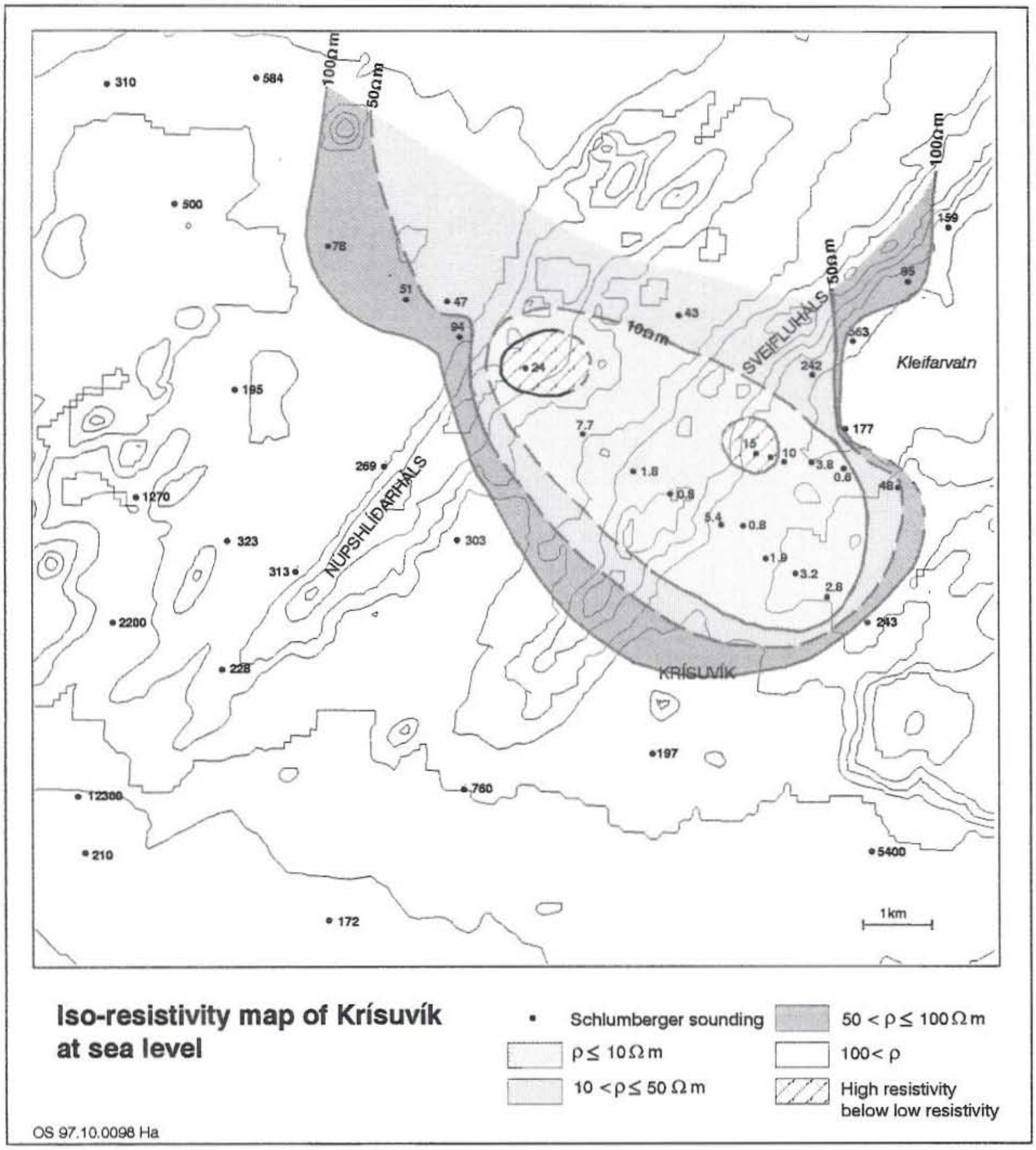

FIGURE 12: Iso-resistivity map of the Krísuvík area at sea level

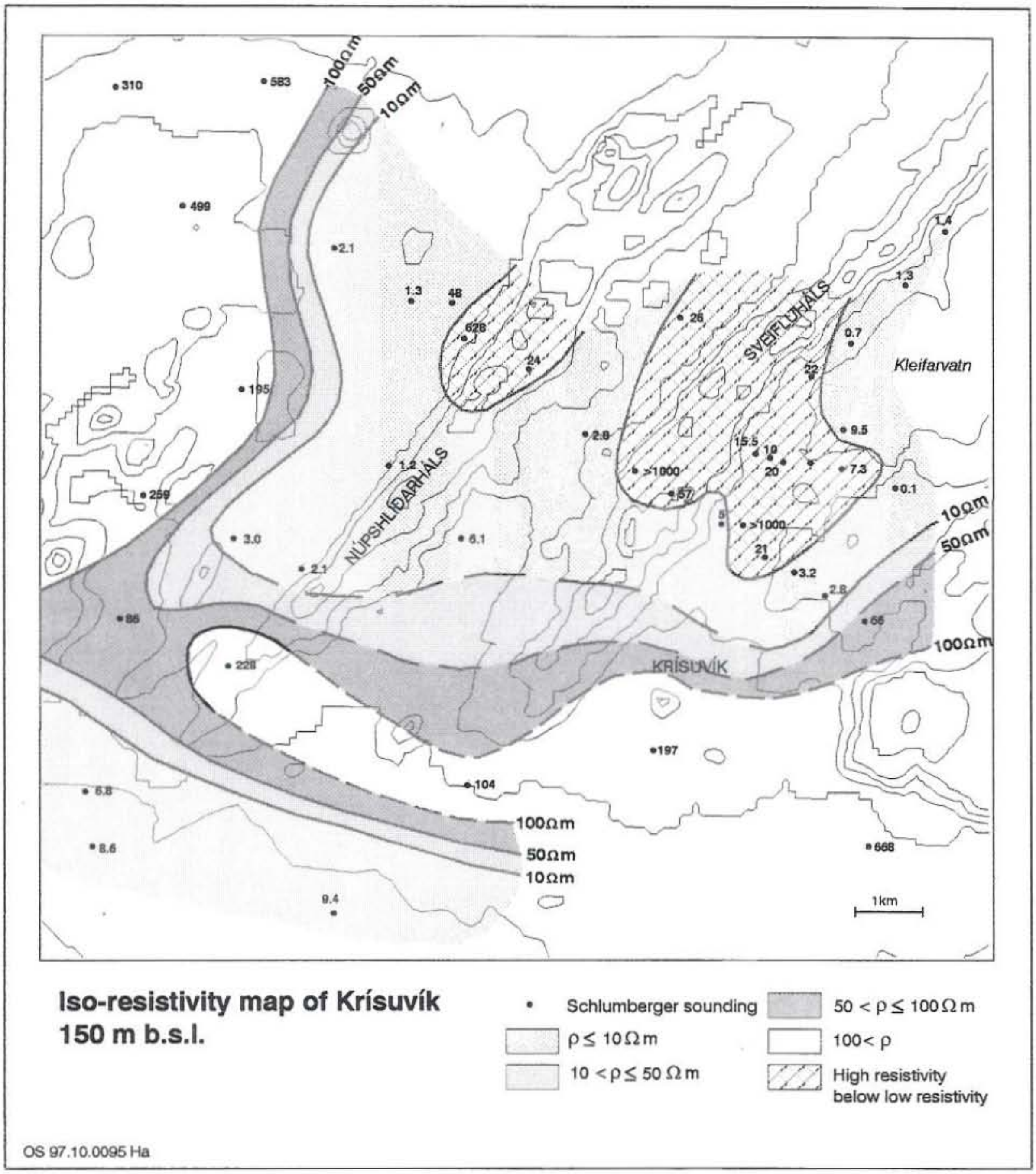

FIGURE 13: Iso-resistivity map of the Krísuvík area at 150 m below sea level

Iso-resistivity map at 150 m b.s.l. (Figure 13). At 150 m below sea level an extensive low-resistivity anomaly is found under most of the northern part of the survey area. The anomaly is bound to the west and south, but not to the northeast, because of lack of data in that direction. The two upflow areas seen at 150 m a.s.l. now stand out as higher resistivity below low-resistivity. An anomaly is seen at the south coast, but this is most likely due to seawater penetration.

Iso-resistivity maps at 300 m and at 500 m b.s.l. (Figures 14 and 15). These maps show the same trend as the other maps. The resistivity anomaly increases in spatial extension with depth. A continuous high resistivity core is found under, and between, the hyaloclastite ridges. Its extension increases with depth and its northeast boundary is not defined because of lack of data.

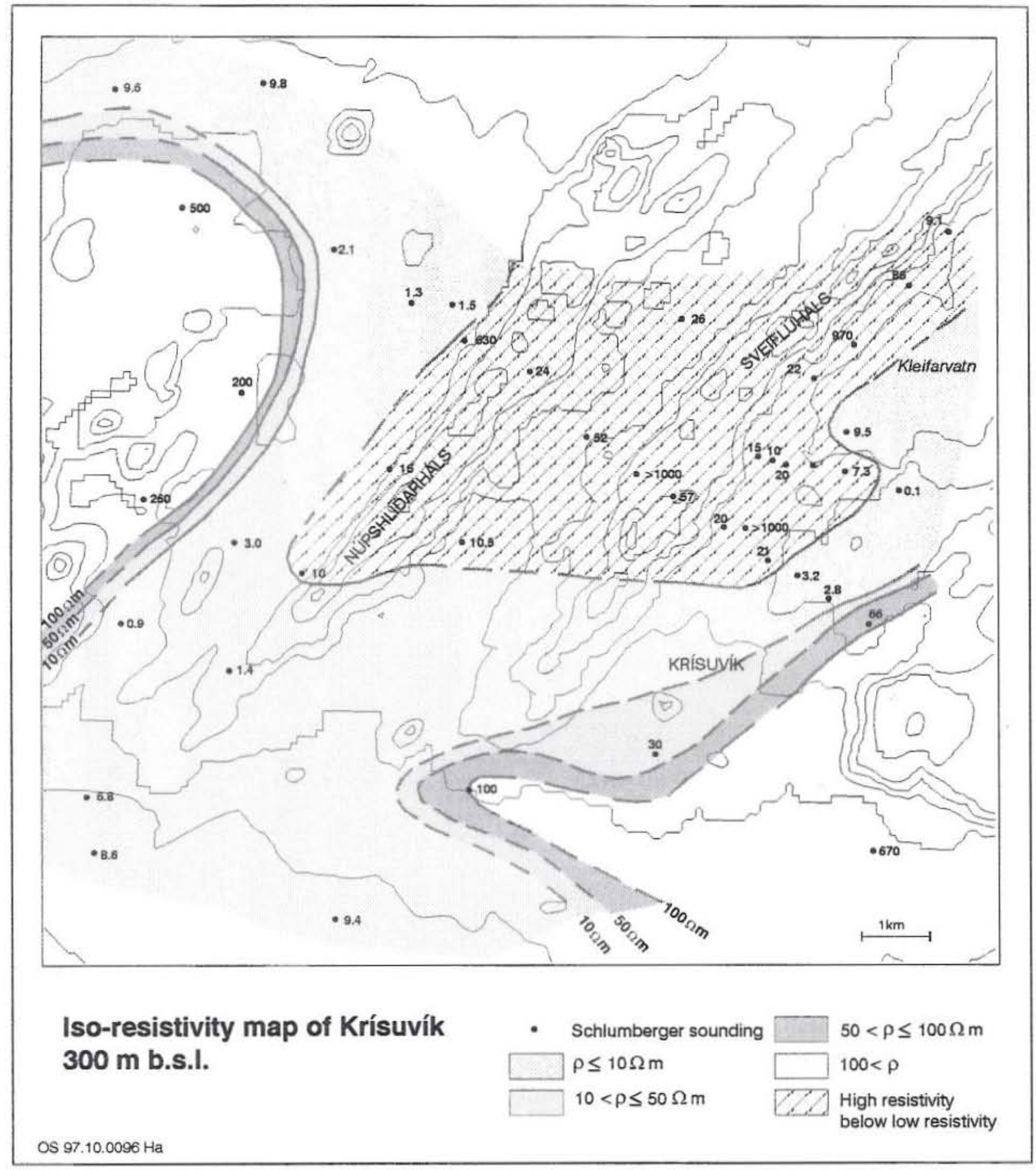

FIGURE 14: Iso-resistivity map of the Krísuvík area at 300 m below sea level

6.5 Discussion of the results

The results of one-dimensional interpretation of 43 soundings reflect the hydrothermal alteration and the geological and structural features in the prospect area. From the resistivity cross-sections and iso-resistivity maps the following can be said.

- A high-resistivity layer at the surface outside the main zone of geothermal activity, with resistivity values higher than 100 Ωm is observed. According to comparison of resistivity structures, alteration mineralogy and temperatures in the geothermal system, this layer reflects cold rocks with temperatures lower than 50°C.

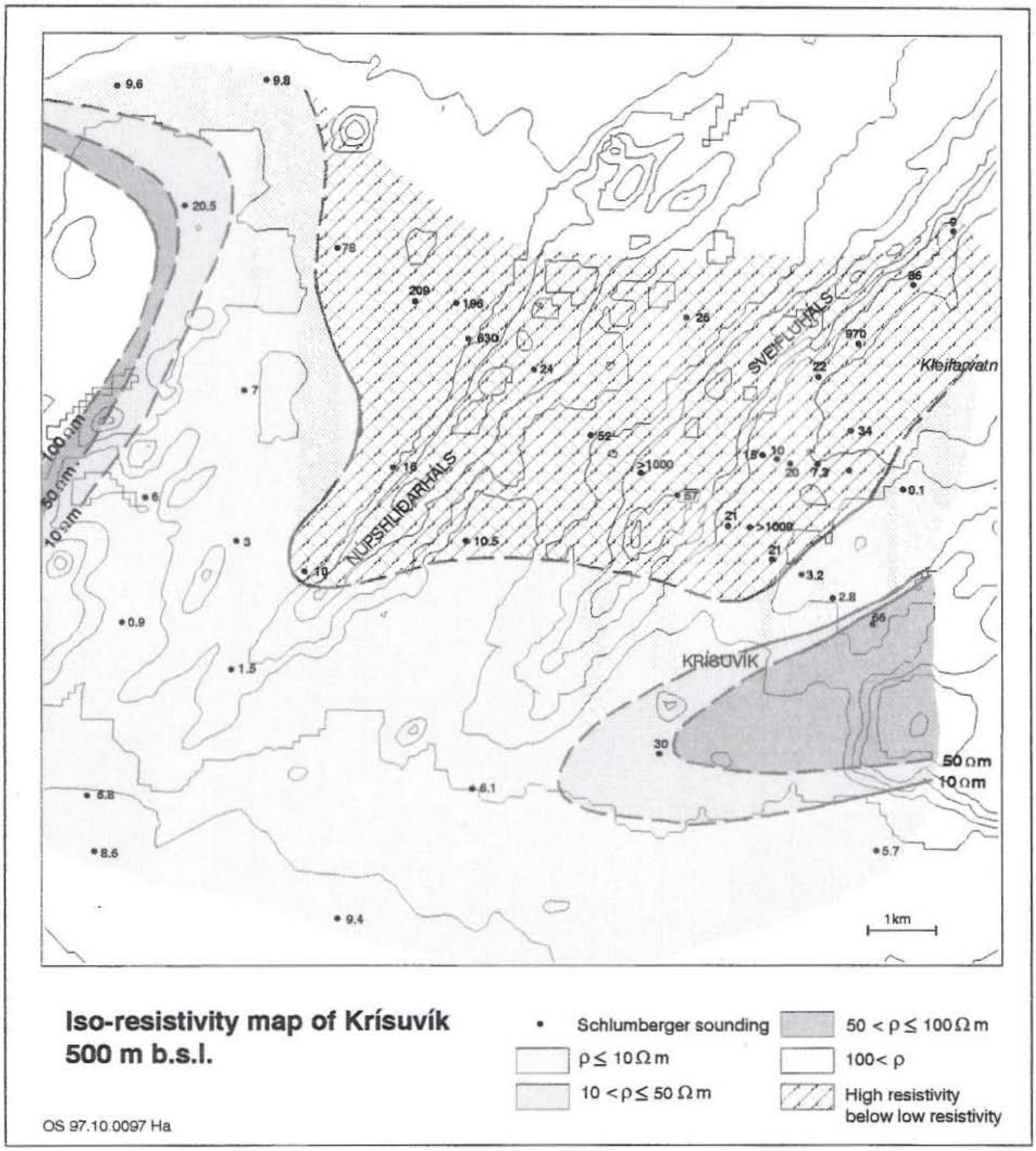

FIGURE 15: Iso-resistivity map of the Krísuvík area at 500 m below sea level

- Below the near-surface resistive rocks, an extensive low-resistivity cap with resistivity values lower than 5 Ωm is observed. This layer reflects temperatures in the range of 50-200°C on the outer margins of the geothermal systems. This layer is found to coincide with the smectite zeolite zone.

- Below the low-resistivity cap, resistivity increases again with resistivity values in the range from 15 to over 10,000 Ωm. The high-resistivity core appears in the mixed-layer clay and chlorite zone, corresponding to temperatures about 240°C or higher inside the geothermal system.

- The iso-resistivity maps show an elongated low-resistivity anomaly trending NW-SE, indicating an outflow zone along the geothermal system. The maps also show the elevation of the top of the low-resistivity cap and the top of the high-resistivity core, suggesting an upflow zone in the southern part of the area which is also supported by high temperatures, and very low resistivity values in the cap. Based on the iso-resistivity at 300 m and 500 m b.s.l., a geothermal system of 42 km² is delineated by the low-resistivity cap and the underlying high-resistivity core.

The resistivity cross-sections and iso-resistivity maps presented here can be interpreted in terms of geothermal activity in a relatively straightforward manner. The resistivity anomaly (low-resistivity cap and the high-resistivity core below low resistivity) in the northern part of the survey area shows where the geothermal activity rises highest in the survey area. The anomaly correlates well with the abundant surface manifestations; it probably shows the top of an upward convecting geothermal plume with temperatures of 240°C and higher. The iso-resistivity map at 500 m below sea level shows that the resistivity anomaly covers a considerably large area and reflects a larger extension of the geothermal system at depth.

6.6 Comparison of TEM data and Schlumberger data

A theoretical overview of the interpretation of TEM sounding using the one-dimensional inversion program TINV is described in Section 4.3. Figures 16 and 17 show a comparison of one-dimensional inversion of TEM soundings (station 4687, 4485) and Schlumberger soundings(station TD084 and TD069A). Each pair of soundings is at the same locations.

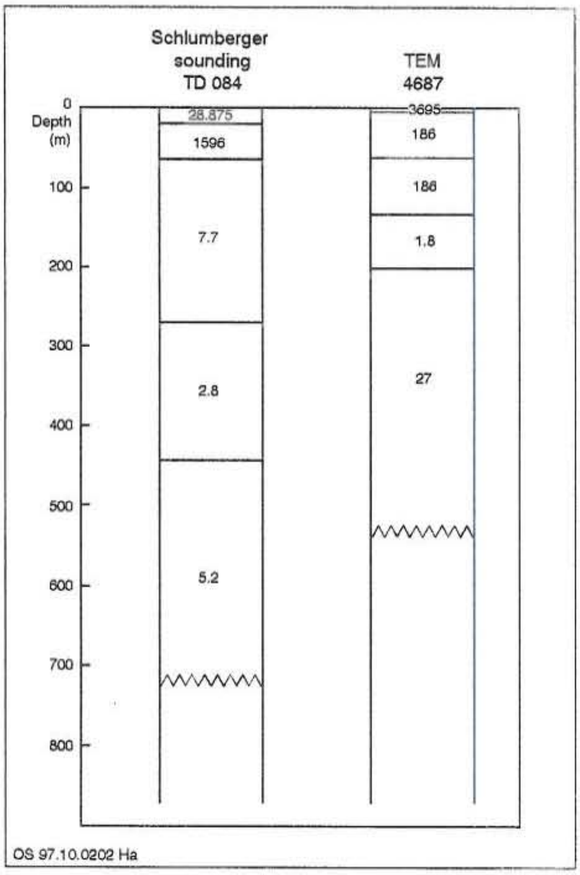

FIGURE 16: Comparison of the results of Schlumberger sounding TD084 and TEM sounding 4687 from the same location

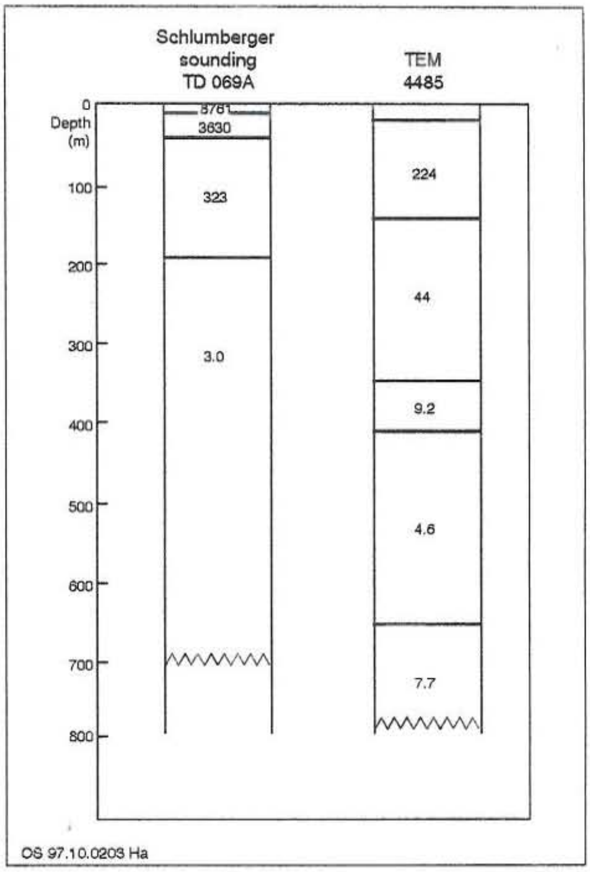

FIGURE 17: Comparison of the results of Schlumberger sounding TD069A and TEM sounding 4485 from the same location

The resistive surface layer is clearly defined by the Schlumberger method while TEM has limited resolution at shallow depth. This is due to the technical limitations of the TEM equipment; it cannot sample transients in the early stage especially for a thick resistive first layer.

The comparisons on Figures 16 and 17 show that the one-dimensional inversion of the Schlumberger and TEM soundings give somewhat different models. The overall structure is mainly the same but details differ considerably. This is a reflection of a fundamental difference between these methods. In the case of Schlumberger soundings, large volumes of rocks, extending over large lateral distances are involved when probing to grade depths. This makes Schlumberger soundings increasingly sensitive to lateral resistivity variations with the depth of exploration. The TEM soundings are more downwardly focussed and, hence, less sensitive to lateral variations. In access with large lateral variations, as is the case in the preceeding examples, both methods will reveal the general structure, but the TEM method is, in general, capable of revealing more details.

Based on general experience, the advantages and disadvantages of the Schlumberger and TEM sounding methods can be summarized as follows:

Andvantages:

- The Schlumberger method has been widely used for a long time and a lot of experience has been obtained, the necessary equipment is relatively simple and cheap. The data collection process is "transparent" in the sense that measured signals can be visually inspected and a skilled operator can recognize anomalous function of equipment and take appropriate measures.
- The TEM method is much more downwardly focussed than the Schlumberger method. This implies that one-dimensional inversion of TEM sounding is much better suited for resolving complicated resistivity structures than that of Schlumberger sounding. The TEM method is relatively insensitive to local resistivity inhomogeneities at the sounding site, which can be a severe problem in Schlumberger soundings.

Disadvantages:

Schlumberger method

- The sounding results can be badly affected by local resistivity anomalies around the receiver dipole.
- The large transmitter dipole, needed for deep soundings, can be a severe problem in areas of difficult topography and dense vegetation.
- In areas with dry and resistive surfaces, transmission of sufficient current to the ground can be a difficult problem.

TEM method

- The data acquisition is highly automatized and not very "transparent". This means that malfunction in the instruments or corrupted data is not as easily recognized as in the more transparent data collection in the Schlumberger soundings.
- The TEM method is based on the recording of transient magnetic fields, and is therefore sensitive to broad band electromagnetic noise. The method is, therefore, hard to apply close to power lines and other places with a lot of electromagnetic noise.

7. CONCLUSIONS

Schlumberger soundings and TEM soundings have been developed to such a stage that they are used routinely in geothermal exploration and Schlumberger soundings have been used for a long time. In routine use, the sounding results are normally interpreted in terms of layered-earth models by one-dimensional inversion. The basic ingredients of the inversion programs for these methods, the solution to the forward problem and inversion algorithms, are well established.

The Schlumberger data (and TEM data) from the Krísuvík geothermal field in SW-Iceland have been interpreted by one-dimensional inversion. The one-dimensional models of the 43 Schlumberger soundings have been used to compile two resistivity cross-sections through the surveyed area and iso-resistivity maps at 150 m a.s.l, sea level, 150, 300 and at 500 m b.s.l. These maps show a clear low-resistivity cap overlying a more resistive core, having the same general structure as found in many other high-temperature geothermal systems in Iceland.

Bedrock resistivity at depth in the Krísuvík area is influenced by the relative position of the water table, water salinity, alteration and underground temperatures. High-resistivity values are predominant at the surface in Postglacial lava fields except in area affected by surficial acid leaching. Widespread low-resistivity layers (<8 Ωm) in the uppermost 500 m correlate with geothermal activity. The low-resistivity cap is underlain by high resistivity. The increased resistivity at depth probably reflects transition in dominant alteration minerals, from smectite to chlorite and epidote which occurs at about 240°C.

Logs from wells in the Krísuvík area show temperature inversion, indicating lateral flow of geothermal waters. This indicates that high resistivity below a low-resistivity layer might, in some places, be caused by decreasing temperature with depth.

Due to limited accessibility, the resistivity data from the Krísuvík area presented in this report is not evenly distributed in the survey area. Some relatively large areas are poorly covered, and more soundings are needed to fill in details of the resistivity structure.

ACKNOWLEDGEMENTS

I am grateful to all the staff of the United Nations University and Orkustofnun, most especially to Dr. Ingvar B. Fridleifsson, director, for the award of the Fellowship to the Geothermal Training Programme, 1997, and to Mr. Lúdvík S. Georgsson and Mrs. Gudrún Bjarnadóttir for their special help and guidance during the training course.

Special thanks go to the geophysicists of Orkustofnun, in particular Knútur Árnason, my adviser, for his unselfish, tireless efforts and willingness to share his professional experience. Thanks to Dr. Hjálmar Eysteinsson, Ragna Karlsdóttir and Karl Gunnarsson for the lectures during the specialised training and field work.

Many thanks to the Geological and Mineral Survey of Vietnam, Hydrogeological Division No.2 for encouragement and the granting of leave to study in this programme. And lastly, but not least, my deepest gratitude is to my wife, Dao Oanh and daughter, Ha Trang, for enduring the long absence from home, and physical separation.

REFERENCES

Archie, G.E., 1942: The electrical resistivity log as an aid in determining some reservoir characteristics. *Tran. AIME, 146,* 54-67.

Árnason, K., 1984: The effect of finite electrode separation on Schlumberger soundings. *54th Annual International SEG Meeting, Atlanta, Expanded Abstracts,* 129-132.

Árnason, K., 1989: *Central loop transient electromagnetic sounding over a horizontally layered earth.* Orkustofnun, Reykjavík, report OS-89032/JHD-06, 129 pp.

Árnason, K., 1990: Central-loop transient electromagnetic soundings in geothermal and groundwater exploration, a step forward. *Geoth. Res. Council, Transactions, 14-II,* 845-850.

Árnason, K., and Flóvenz, Ó.G., 1992: Evaluation of physical methods in geothermal exploration of rifted volcanic crust. *Geoth. Res. Council, Transactions, 16,* 207-214.

Árnason, K., and Hersir, G.P., 1988: *One-dimensional inversion of Schlumberger resistivity soundings. Computer program, description and user's guide.* UNU G.T.P., Iceland, report 8, 59 pp.

Arnórsson, S., Björnsson, A., Björnsson, S., Einarsson, P., Gíslason, G., Gudmundsson, G., Gunnlaugsson, E., Jónsson, J., and Sigurmundsson, S.G, 1975: *The Krísuvík area. A complete report on geothermal exploration.* Orkustofnun, Reykjavík, report OS JHD-7554 (in Icelandic), 71 pp + figures.

Flóvenz, Ó.G., 1984: Application of the head-on resistivity profiling method in geothermal exploration. *Geoth. Res., Council, Transactions, 18,* 493-498.

Fox, R.C., Hohmann, G.W., and Rijo, L., 1978: *Topographic effects in resistivity surveys* Earth Science Laboratory, Salt Lake City, Utah, report, 99 pp.

Georgsson, L.S., 1987: Application of resistivity sounding in the exploration of high-temperature geothermal areas in Iceland with examples from the Trölladyngja-Krýsuvík area, SW-Iceland. *Technical Programme and Abstracts of Exploration '87, Toronto,* 52.

Hersir, G.P., and Björnsson, A., 1991: *Geophysical exploration for geothermal resources. Principles and applications.* UNU G.T.P., Iceland, report 15, 94 pp.

Hochstein, M.P., and Soengkono, 1995: *Geothermal exploration for earth scientists.* Universtity of Auckland, Geothermal Institute, Unpublished lecture notes.

Johansen H.K., 1977: A man/computer interpretation system for resistivity soundings over a horizontally stratified earth. *Geophys. Prosp. 25,* 667-691.

Orkustofnun and Vatnaskil Consulting Engineers, 1986: *Vatnsleysa-Trölladyngja, freshwater and geothermal investigation.* Orkustofnun, Reykjavík, report OS-86032/JHD-10B, 92 pp and maps.

Saemundsson, K., and Fridleifsson, I.B., 1980: Application of geology in geothermal research in Iceland. *Náttúrufraedingurinn, 50* (in Icelandic with English summary), 157-188.

Vargas M, J.R., 1992: *Geology and geothermal considerations of Krísuvík valley, Reykjanes, Iceland.* UNU G.T.P., Iceland, report 13, 35 pp.

APPENDIX I: The measured Schlumberger resistivity curves, interpreted data curves and layered resistivity models from the Krísuvík geothermal area

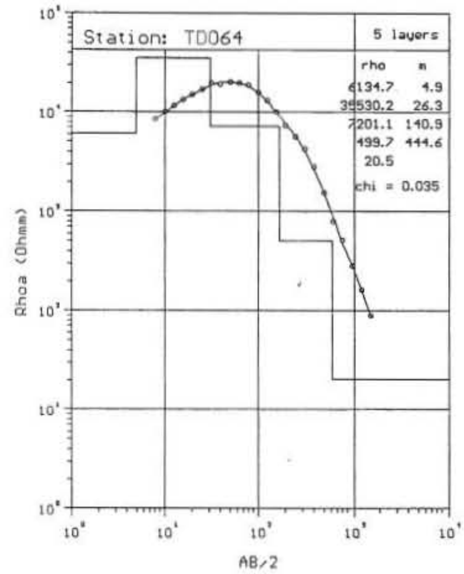

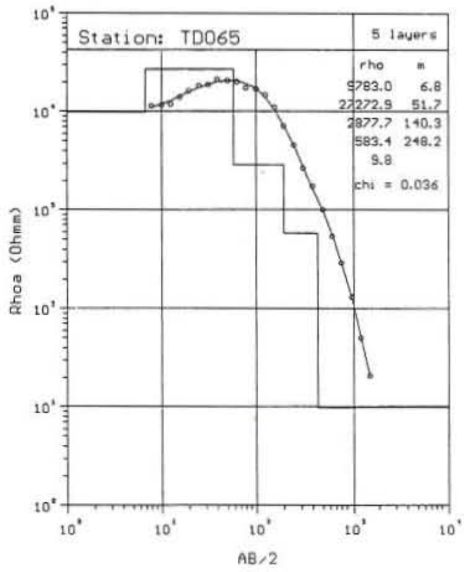

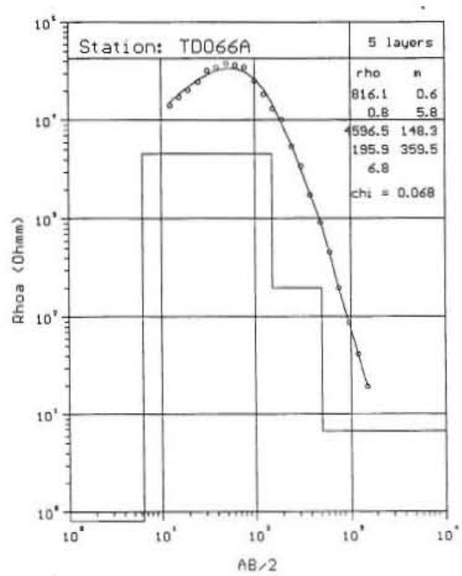

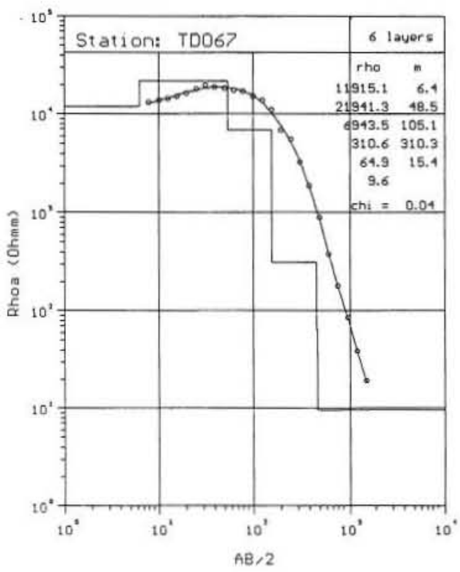

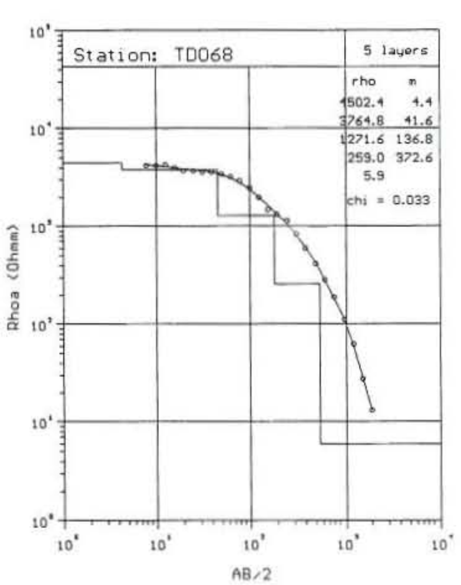

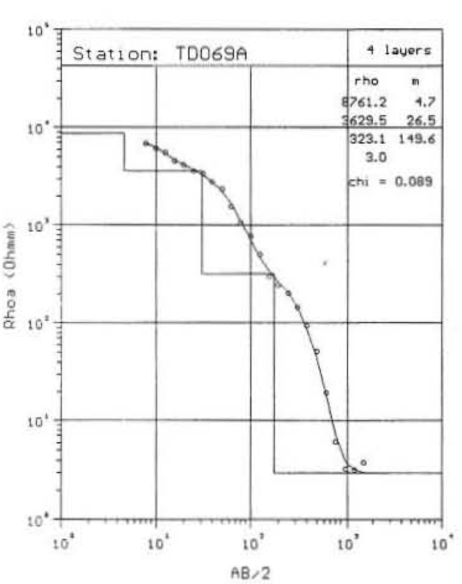

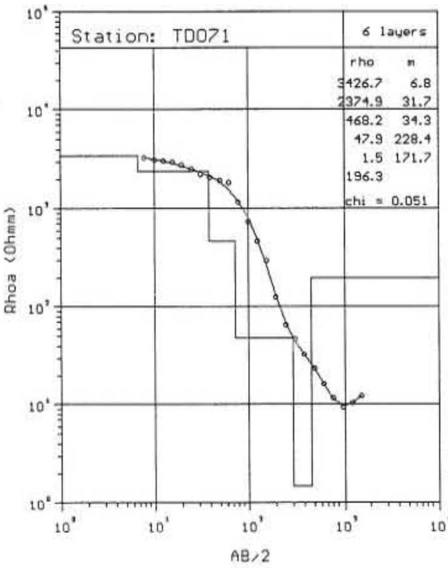
Station: TD071
6 layers
rho m
3426.7 6.8
2374.9 31.7
468.2 34.3
47.9 228.4
1.5 171.7
196.3
chi = 0.051
Rhoa (Ohmm)
10^0
10^1
10^2
10^3
10^4
10^5
AB/2

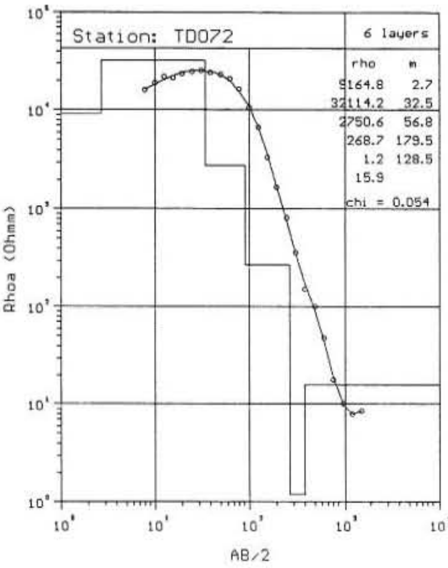
Station: TD072
6 layers
rho m
9164.8 2.7
32114.2 32.5
2750.6 56.8
268.7 179.5
1.2 128.5
15.9
chi = 0.054
Rhoa (Ohmm)
10^0
10^1
10^2
10^3
10^4
10^5
AB/2

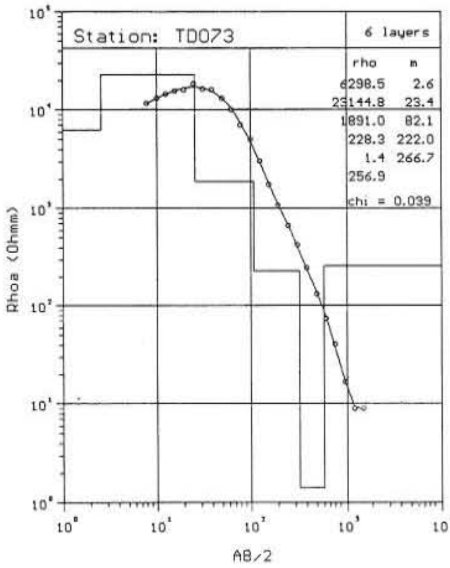
Station: TD073
6 layers
rho m
6298.5 2.6
23144.8 23.4
1891.0 82.1
228.3 222.0
1.4 266.7
256.9
chi = 0.039
Rhoa (Ohmm)
10^0
10^1
10^2
10^3
10^4
10^5
AB/2

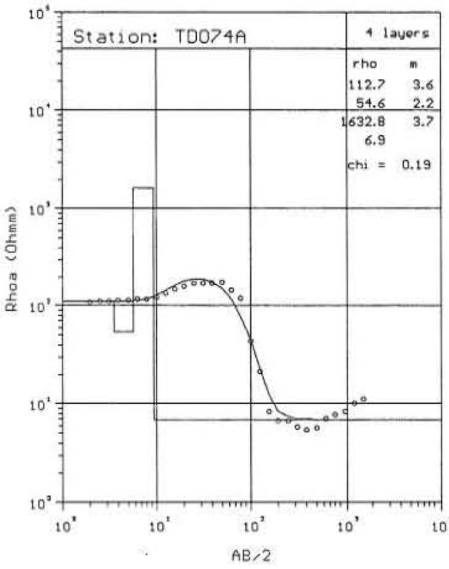
Station: TD074A
4 layers
rho m
112.7 3.6
54.6 2.2
1632.8 3.7
6.9
chi = 0.19
Rhoa (Ohmm)
10^0
10^1
10^2
10^3
10^4
10^5
AB/2

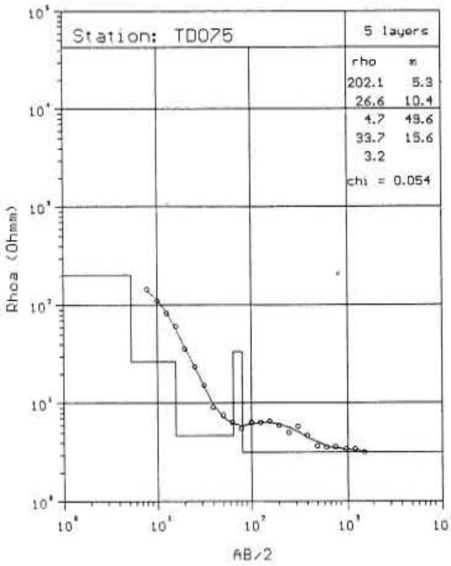
Station: TD075
5 layers
rho m
202.1 5.3
26.6 10.4
4.7 49.6
33.7 15.6
3.2
chi = 0.054
Rhoa (Ohmm)
10^0
10^1
10^2
10^3
10^4
10^5
AB/2

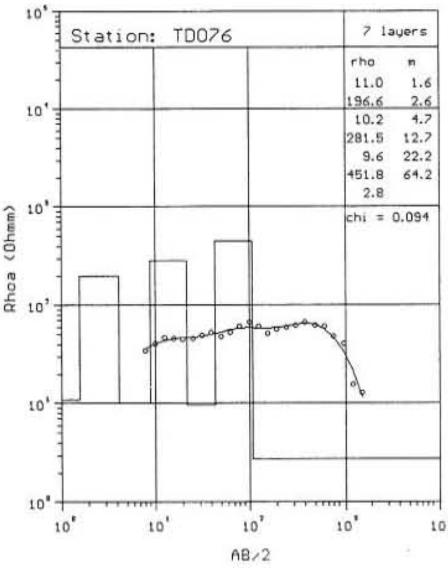
Station: TD076
7 layers
rho m
11.0 1.6
196.6 2.6
10.2 4.7
281.5 12.7
9.6 22.2
451.8 64.2
2.8
chi = 0.094
Rhoa (Ohmm)
10^0
10^1
10^2
10^3
10^4
10^5
AB/2

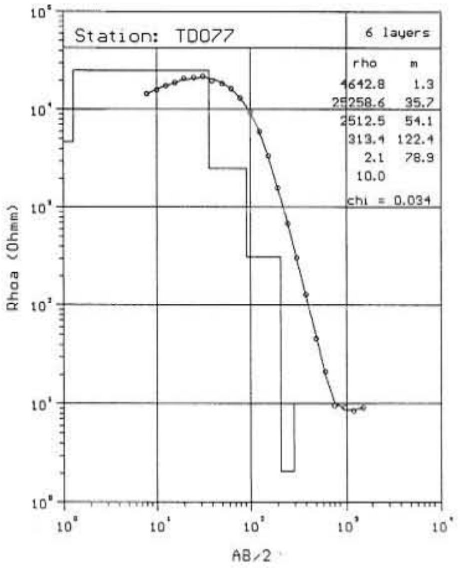
Station: TD077
6 layers
rho m
4642.8 1.3
25258.6 35.7
2512.5 54.1
313.4 122.4
2.1 78.9
10.0
chi = 0.034
Rhoa (Ohmm)
AB/2
10^0
10^1
10^2
10^3
10^4
10^5

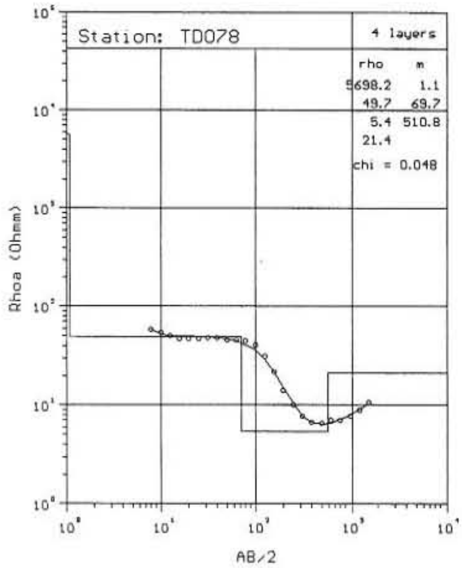
Station: TD078
4 layers
rho m
5698.2 1.1
49.7 69.7
5.4 510.8
21.4
chi = 0.048
Rhoa (Ohmm)
AB/2
10^0
10^1
10^2
10^3
10^4
10^5

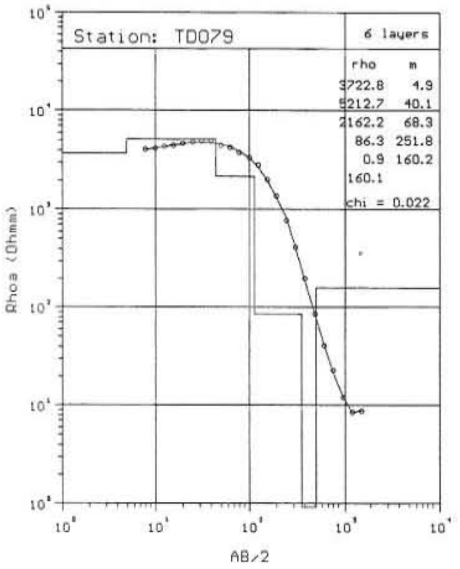
Station: TD079
6 layers
rho m
3722.8 4.9
5212.7 40.1
2162.2 68.3
86.3 251.8
0.9 160.2
160.1
chi = 0.022
Rhoa (Ohmm)
AB/2
10^0
10^1
10^2
10^3
10^4
10^5

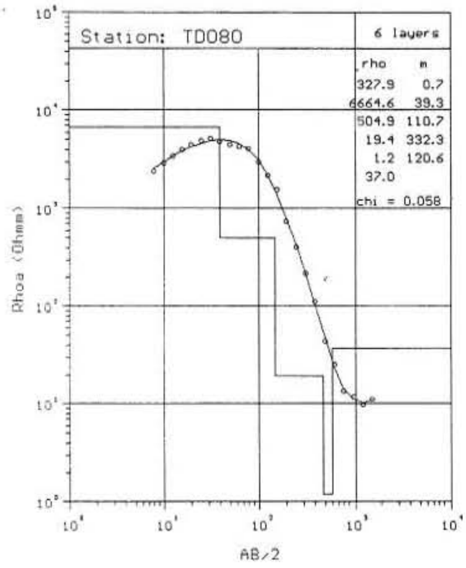
Station: TD080
6 layers
rho m
327.9 0.7
6664.6 39.3
504.9 110.7
19.4 332.3
1.2 120.6
37.0
chi = 0.058
Rhoa (Ohmm)
AB/2
10^0
10^1
10^2
10^3
10^4
10^5

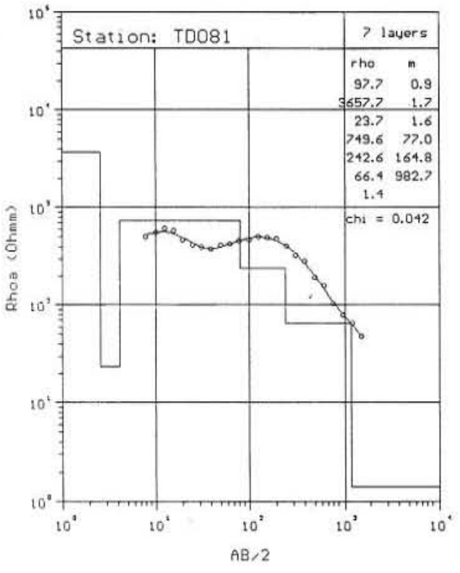
Station: TD081
7 layers
rho m
97.7 0.9
3657.7 1.7
23.7 1.6
749.6 77.0
242.6 164.8
66.4 982.7
1.4
chi = 0.042
Rhoa (Ohmm)
AB/2
10^0
10^1
10^2
10^3
10^4
10^5

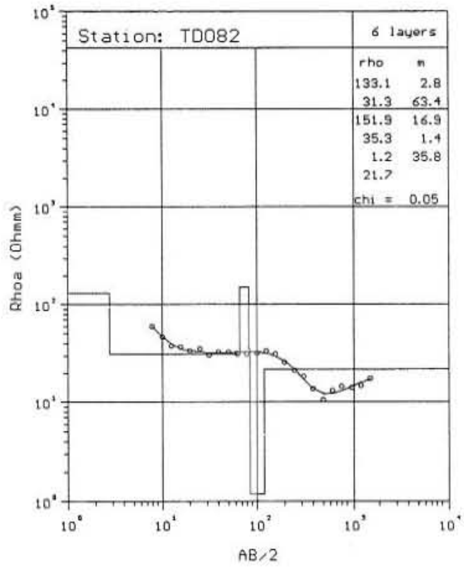
Station: TD082
6 layers
rho m
133.1 2.8
31.3 63.4
151.9 16.9
35.3 1.4
1.2 35.8
21.7
chi = 0.05
Rhoa (Ohmm)
AB/2
10^0
10^1
10^2
10^3
10^4
10^5

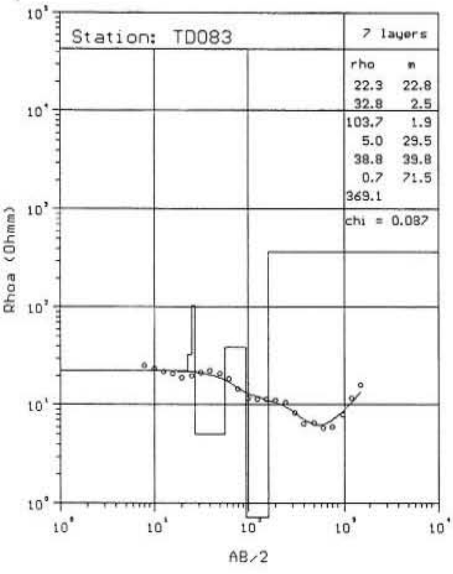
Station: TD083
7 layers
rho m
22.3 22.8
32.8 2.5
103.7 1.9
5.0 29.5
38.8 39.8
0.7 71.5
369.1
chi = 0.087
Rhoa (Ohmm)
10^0
10^1
10^2
10^3
10^4
10^5
10^0
10^1
10^2
10^3
10^4
AB/2

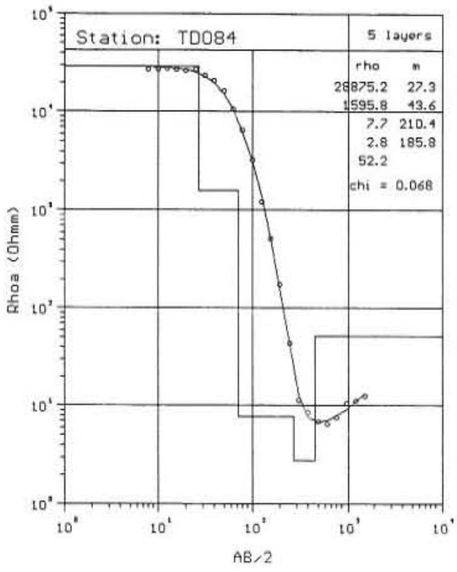
Station: TD084
5 layers
rho m
28875.2 27.3
1595.8 43.6
7.7 210.4
2.8 185.8
52.2
chi = 0.068
Rhoa (Ohmm)
10^0
10^1
10^2
10^3
10^4
10^5
10^0
10^1
10^2
10^3
10^4
AB/2

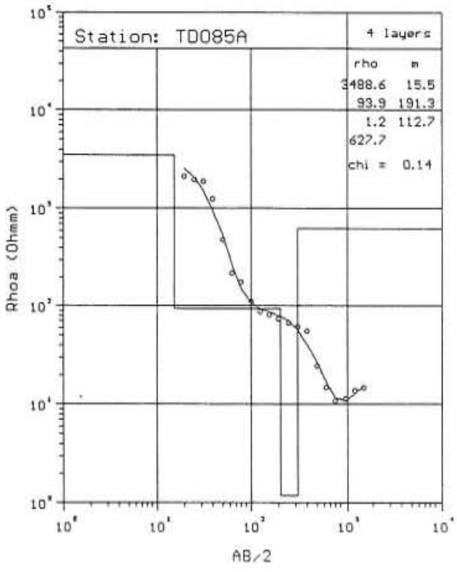
Station: TD085A
4 layers
rho m
3488.6 15.5
93.9 191.3
1.2 112.7
627.7
chi = 0.14
Rhoa (Ohmm)
10^0
10^1
10^2
10^3
10^4
10^5
10^0
10^1
10^2
10^3
10^4
AB/2

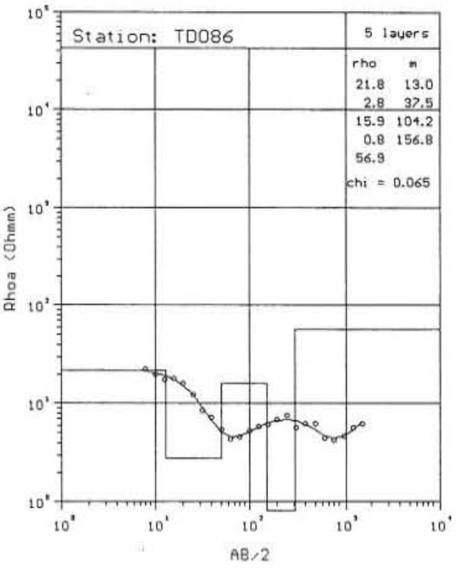
Station: TD086
5 layers
rho m
21.8 13.0
2.8 37.5
15.9 104.2
0.8 156.8
56.9
chi = 0.065
Rhoa (Ohmm)
10^0
10^1
10^2
10^3
10^4
10^5
10^0
10^1
10^2
10^3
10^4
AB/2

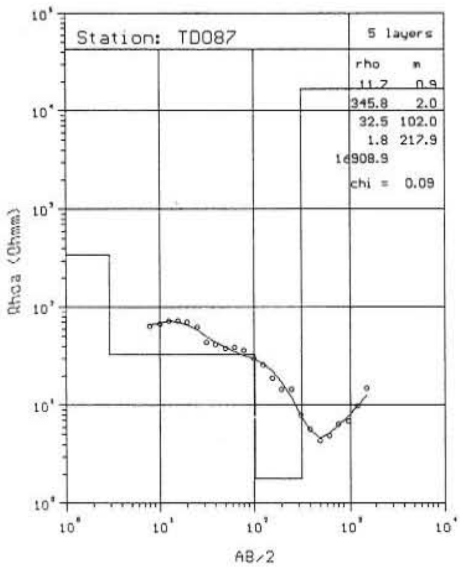
Station: TD087
5 layers
rho m
11.7 0.9
345.8 2.0
32.5 102.0
1.8 217.9
16908.9
chi = 0.09
Rhoa (Ohmm)
10^0
10^1
10^2
10^3
10^4
10^5
10^0
10^1
10^2
10^3
10^4
AB/2

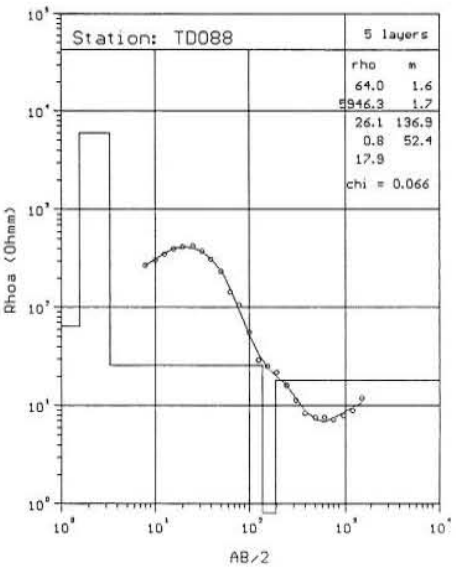
Station: TD088
5 layers
rho m
64.0 1.6
5946.3 1.7
26.1 136.9
0.8 52.4
17.9
chi = 0.066
Rhoa (Ohmm)
10^0
10^1
10^2
10^3
10^4
10^5
10^0
10^1
10^2
10^3
10^4
AB/2

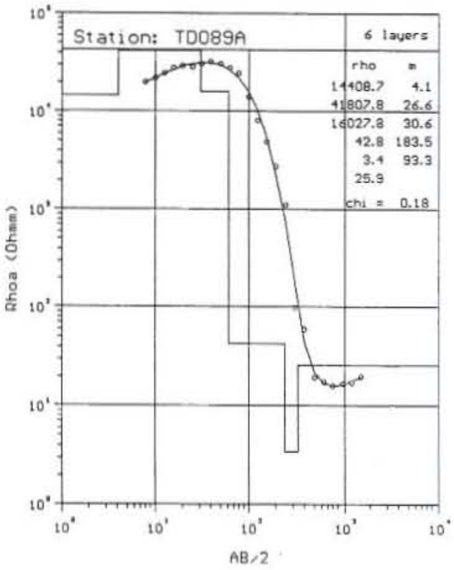
Station: TD089A
6 layers
rho m
14408.7 4.1
41807.8 26.6
16027.8 30.6
42.8 183.5
3.4 93.3
25.9
chi = 0.18
Rhoa (Ohmm)
10^5
10^4
10^3
10^2
10^1
10^0
10^0
10^1
10^2
10^3
10^4
AB/2

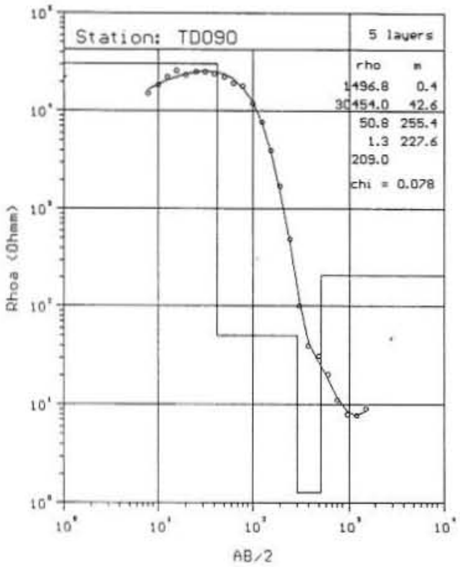
Station: TD090
5 layers
rho m
1496.8 0.4
30454.0 42.6
50.8 255.4
1.3 227.6
209.0
chi = 0.078
Rhoa (Ohmm)
10^5
10^4
10^3
10^2
10^1
10^0
10^0
10^1
10^2
10^3
10^4
AB/2

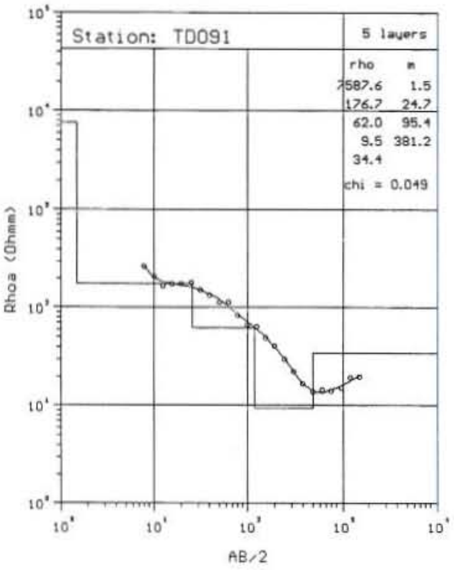
Station: TD091
5 layers
rho m
7587.6 1.5
176.7 24.7
62.0 95.4
9.5 381.2
34.4
chi = 0.049
Rhoa (Ohmm)
10^5
10^4
10^3
10^2
10^1
10^0
10^0
10^1
10^2
10^3
10^4
AB/2

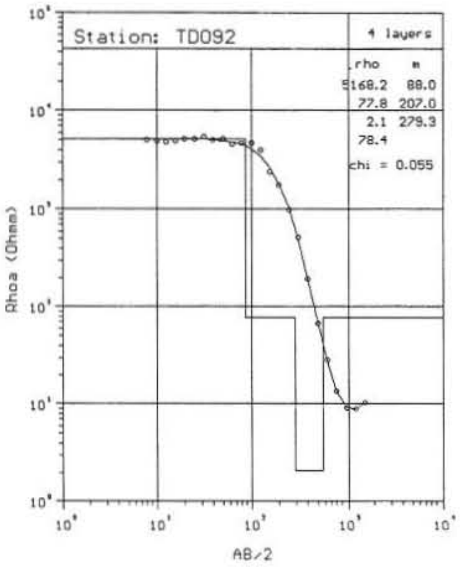
Station: TD092
4 layers
rho m
5168.2 88.0
77.8 207.0
2.1 279.3
78.4
chi = 0.055
Rhoa (Ohmm)
10^5
10^4
10^3
10^2
10^1
10^0
10^0
10^1
10^2
10^3
10^4
AB/2

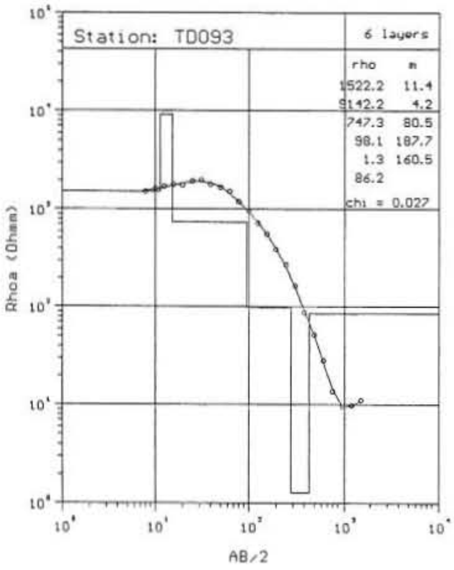
Station: TD093
6 layers
rho m
1522.2 11.4
9142.2 4.2
747.3 80.5
98.1 187.7
1.3 160.5
86.2
chi = 0.027
Rhoa (Ohmm)
10^5
10^4
10^3
10^2
10^1
10^0
10^0
10^1
10^2
10^3
10^4
AB/2

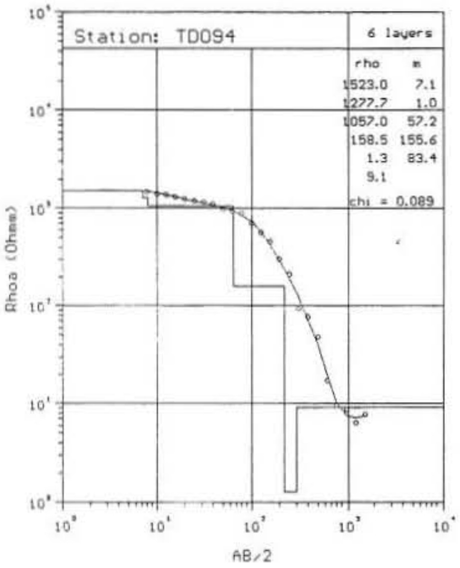
Station: TD094
6 layers
rho m
1523.0 7.1
1277.7 1.0
1057.0 57.2
158.5 155.6
1.3 83.4
9.1
chi = 0.089
Rhoa (Ohmm)
10^5
10^4
10^3
10^2
10^1
10^0
10^0
10^1
10^2
10^3
10^4
AB/2

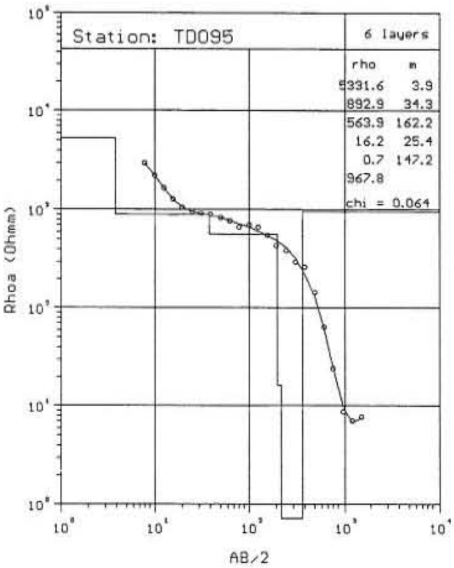
Station: TD095
6 layers
rho m
5331.6 3.9
892.9 34.3
563.9 162.2
16.2 25.4
0.7 147.2
967.8
chi = 0.064
Rhoa (Ohmm)
AB/2
10⁰
10¹
10²
10³
10⁴
10⁵

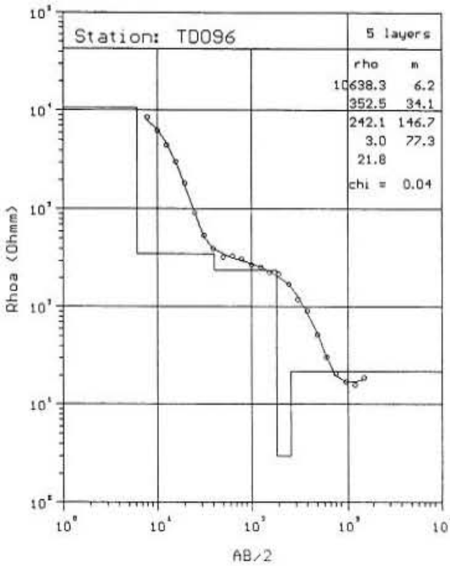
Station: TD096
5 layers
rho m
10638.3 6.2
352.5 34.1
242.1 146.7
3.0 77.3
21.8
chi = 0.04
Rhoa (Ohmm)
AB/2
10⁰
10¹
10²
10³
10⁴
10⁵

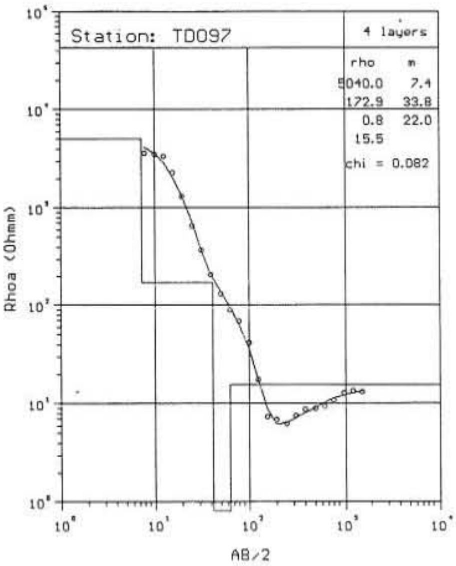
Station: TD097
4 layers
rho m
5040.0 7.4
172.9 33.8
0.8 22.0
15.5
chi = 0.082
Rhoa (Ohmm)
AB/2
10⁰
10¹
10²
10³
10⁴
10⁵

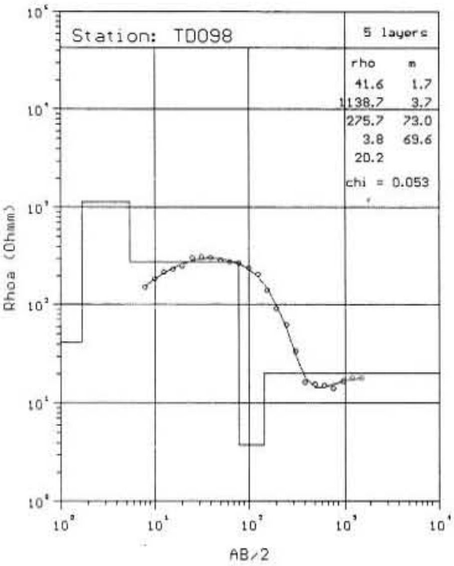
Station: TD098
5 layers
rho m
41.6 1.7
1138.7 3.7
275.7 73.0
3.8 69.6
20.2
chi = 0.053
Rhoa (Ohmm)
AB/2
10⁰
10¹
10²
10³
10⁴
10⁵

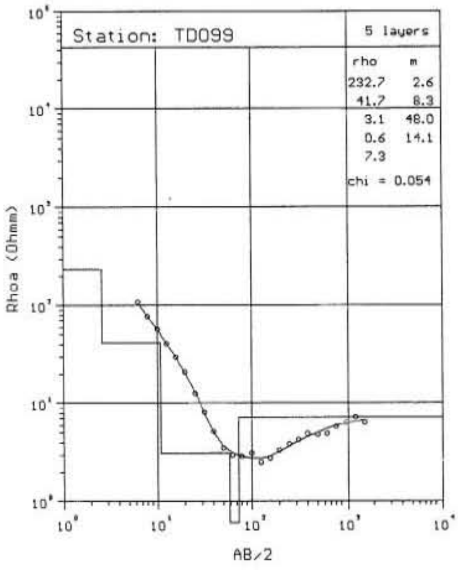
Station: TD099
5 layers
rho m
232.7 2.6
41.7 8.3
3.1 48.0
0.6 14.1
7.3
chi = 0.054
Rhoa (Ohmm)
AB/2
10⁰
10¹
10²
10³
10⁴
10⁵

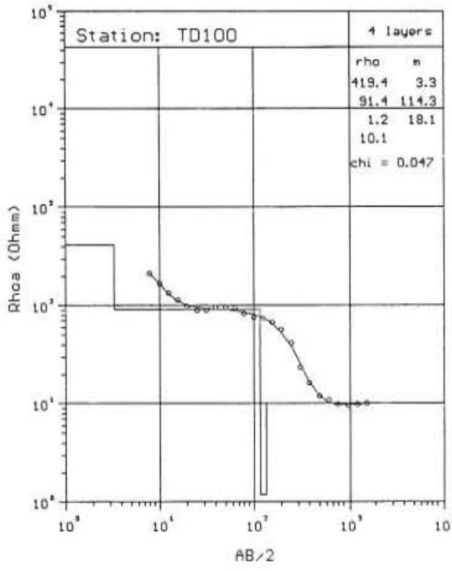
Station: TD100
4 layers
rho m
419.4 3.3
91.4 114.3
1.2 18.1
10.1
chi = 0.047
Rhoa (Ohmm)
AB/2
10⁰
10¹
10²
10³
10⁴
10⁵

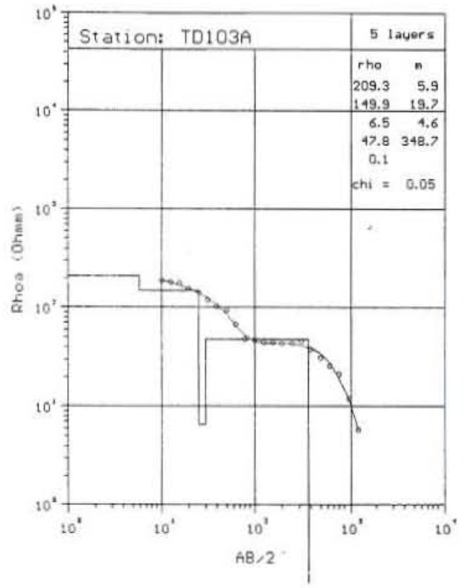
Station: TD103A
5 layers
rho m
209.3 5.9
149.9 19.7
6.5 4.6
47.8 348.7
0.1
chi = 0.05
Rhoa (Ohmm)
AB/2
10^0
10^1
10^2
10^3
10^4
10^5

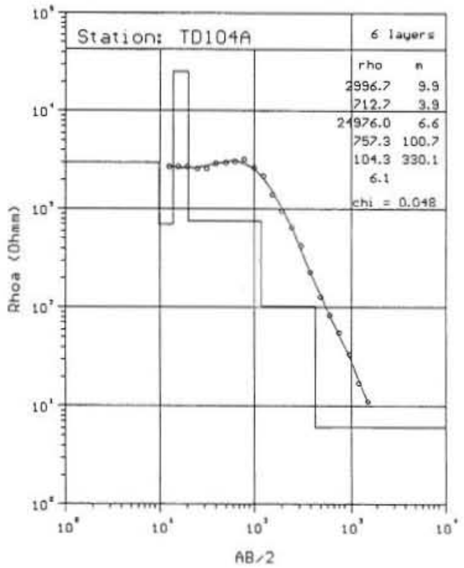
Station: TD104A
6 layers
rho m
2996.7 9.9
712.7 3.9
24976.0 6.6
757.3 100.7
104.3 330.1
6.1
chi = 0.048
Rhoa (Ohmm)
AB/2
10^0
10^1
10^2
10^3
10^4
10^5

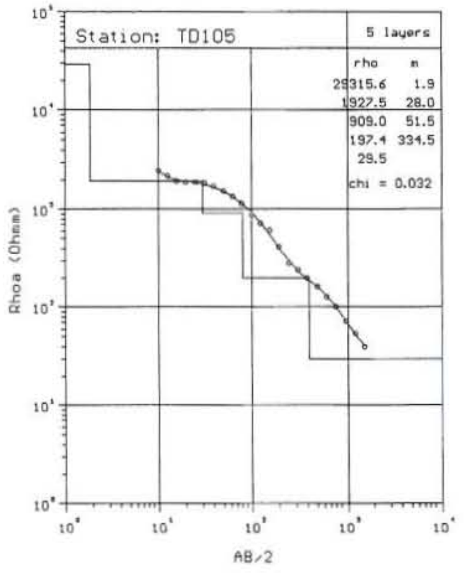
Station: TD105
5 layers
rho m
29315.6 1.9
1927.5 28.0
909.0 51.5
197.4 334.5
29.5
chi = 0.032
Rhoa (Ohmm)
AB/2
10^0
10^1
10^2
10^3
10^4
10^5

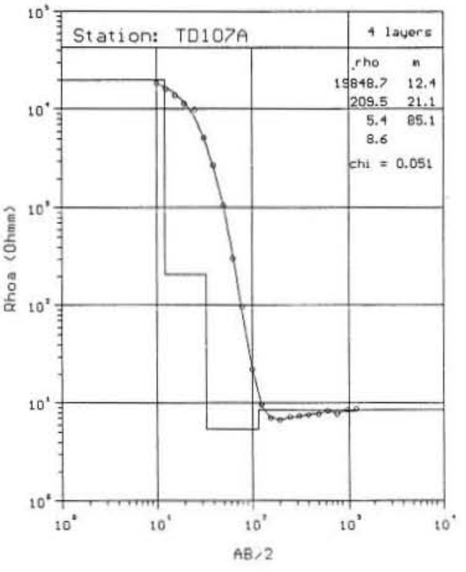
Station: TD107A
4 layers
rho m
19848.7 12.4
209.5 21.1
5.4 85.1
8.6
chi = 0.051
Rhoa (Ohmm)
AB/2
10^0
10^1
10^2
10^3
10^4
10^5

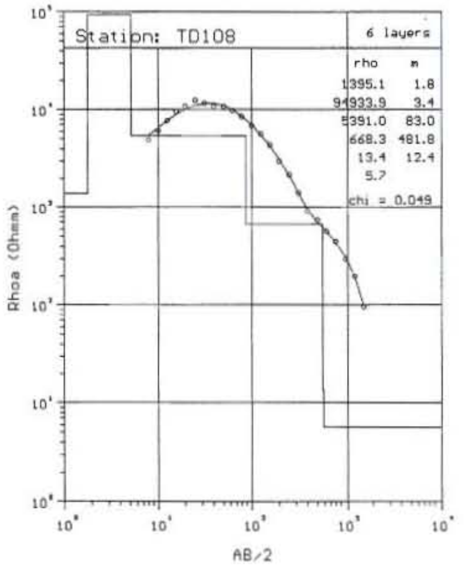
Station: TD108
6 layers
rho m
1395.1 1.8
94933.9 3.4
5391.0 83.0
668.3 481.8
13.4 12.4
5.7
chi = 0.049
Rhoa (Ohmm)
AB/2
10^0
10^1
10^2
10^3
10^4
10^5

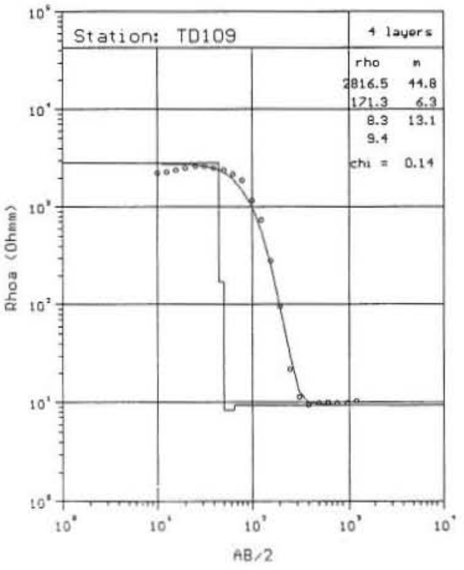
Station: TD109
4 layers
rho m
2816.5 44.8
171.3 6.3
8.3 13.1
9.4
chi = 0.14
Rhoa (Ohmm)
AB/2
10^0
10^1
10^2
10^3
10^4
10^5

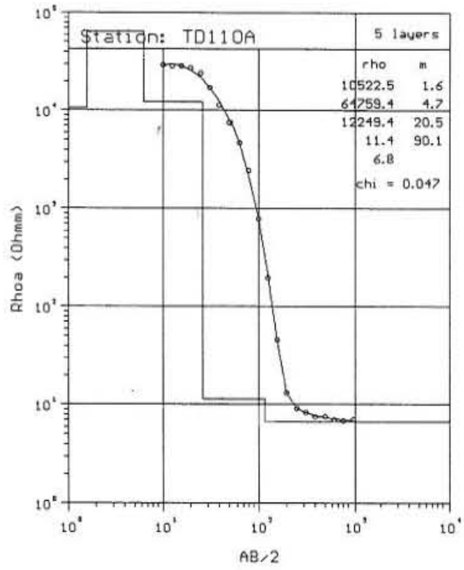

APPENDIX II: The measured TEM resistivity curves, interpreted data curves and layered resistivity models from the Krísuvík geothermal area